The INtegrated CAtchment model of phosphorus dynamics (INCA-P)

Jackson-Blake, L. A. ; Wade, A. J.; Futter, M. N.; Butterfield, D.; Couture, R.-M.; Cox, B. A.

Published in:
Environmental Modelling and Software

DOI:
10.1016/j.envsoft.2016.05.022

Publication date:
2016

The INtegrated CAtchment model of Phosphorus dynamics (INCA-P): description and demonstration of new model structure and equations

Jackson-Blake, LA[a,b]*; Wade, AJ[c]; Futter, MN[d]; Butterfield, D[e]; Couture, R-M[b]; Cox, B.A.[c,f]; Crossman, J[g]; Ekholm, P[h]; Halliday, SJ[c]; Jin, L[i]; Lawrence, DSL[j]; Lepistö, A[h]; Lin, Y[b]; Rankinen, K[h]; Whitehead, PG[k]

[a] The James Hutton Institute, Macaulay Drive, Aberdeen, Scotland, AB15 8QH
[b] Norwegian Institute for Water Research (NIVA), Gaustadaleen 21, 0349, Oslo, Norway
[c] Department of Geography and Environmental Science, University of Reading, RG6 6DW, UK
[d] Department of Aquatic Science and Assessment, Swedish University of Agricultural Sciences, Uppsala, Sweden
[e] ENMOSYS, Vermont, USA
[f] Atkins Limited, Warrington, UK
[g] Chemical Sciences, Trent University, Peterborough, Ontario, Canada
[h] Finnish Environment Institute (SYKE), Helsinki, Finland
[i] Department of Geology, SUNY Cortland, Cortland County, NY 13045 USA
[j] Norwegian Water Resources and Energy Directorate (NVE), Oslo, Norway
[k] School of Geography and the Environment, University of Oxford, UK

*Corresponding author: E-mail: ljb@niva.no. Tel: +47 98227794

Abstract

INCA-P is a dynamic, catchment-scale phosphorus model which has been widely applied during the last decade. Since its original release in 2002, the model structure and equations have been significantly altered during several development phases. Here, we provide the first full model description since 2002 and then test the latest version of the model (v1.4.4) in a small rural catchment in northeast Scotland. The particulate phosphorus simulation was much improved compared to previous model versions, whilst the latest sorption equations allowed us to explore the potential time lags between reductions in terrestrial inputs and improvements in surface water quality, an issue of key policy relevance. The model is particularly suitable for use as a research tool, but should only be used to inform policy and land management in data-rich areas, where parameters and processes can be well-constrained. More long-term data is needed to parameterise dynamic models and test their predictions.

Keywords: phosphorus; process-based; model; catchment; watershed; water quality

1. Introduction

Eutrophication of freshwaters due to excessive anthropogenic inputs of nitrogen and phosphorus (P) is a global problem (e.g. Elser et al., 2007), and reducing P concentrations in surface waters has become a top priority in many areas. Across Europe, marked decreases in dissolved P concentrations in rivers have been seen during the last two decades (around 3 μg l^{-1} per year), driven largely by improvements in wastewater treatment and reductions in detergent P content (EEA, 2015). However, many surface waters still suffer from P-related eutrophication due to both sewage effluent and agricultural P inputs. Across Europe, for example, diffuse P inputs from agriculture are a significant pressure in 50% of surface water bodies (EEA, 2012). To

achieve further reductions in surface water P concentrations, reductions in both point and diffuse P inputs are therefore needed. Effective management of diffuse P sources is particularly difficult: in-stream P concentration is the result of a variety of input fluxes and processes, many of which are highly variable spatially and temporally, meaning there is often no straightforward link between P inputs on land and in-stream P concentrations. In particular, the long-term accumulation of P in catchment soils, groundwater and stream bed sediments may continue to affect freshwater ecology long after farm or effluent-based remediation has been implemented (Jarvie et al., 2013; Meals et al., 2010; Sharpley et al., 2013).

Dynamic, process-based integrated catchment models provide a means of formalising current knowledge of complex catchment systems, and can therefore be useful catchment management tools. Models can be used to highlight knowledge and data gaps and to help design monitoring strategies (e.g. Jackson-Blake and Starrfelt, 2015; McIntyre and Wheater, 2004). Once shown to capture the dominant modes of behaviour in a system, models can provide scientifically-based evidence to support decision-making; for example, to help set appropriate water quality and load reduction goals, to advise on the best means of achieving those goals, to predict time lags and trade-offs in the system, and to explore potential system responses to future environmental change.

Many catchment-scale P models have been developed during the last few decades. Here, we describe the latest version of the INtegrated CAtchment model of Phosphorus dynamics (INCA-P) which, together with SWAT, AGNPS/AnnAGNPS, HSPF and HBV-NP (now superseded by HYPE), is one of the most popular catchment water quality models used worldwide (Wellen et al., 2015). INCA-P is a semi-distributed, process-based, mass-balance model that simulates the daily dynamics of P transport in catchments. During the last decade, INCA-P has been applied to catchments throughout Europe (e.g. Couture et al., 2014; Farkas et al., 2013; Martin-Ortega et al., 2015; Starrfelt and Kaste, 2014; Wade et al., 2007; Wade et al., 2002b; Whitehead et al., 2013), Canada (Baulch et al., 2013; Crossman et al., 2013; Jin et al., 2013) and more recently India (Jin et al., 2015), to explore how P dynamics may respond to changes in land use, land management and climate.

The original version of INCA-P (Wade et al., 2002a) used the same conceptual structure as the nitrogen version of the model, INCA-N (Wade et al., 1999; Whitehead et al., 1998), incorporating the in-stream P dynamics of the Kennet model (Wade et al., 2002b). The model was then tested across a range of European catchments as part of the EU Eurolimpacs project (http://www.refresh.ucl.ac.uk/eurolimpacs). These applications highlighted the need for a number of improvements, and major revisions to the model structure were undertaken. Key changes included: (1) the incorporation of physically-based soil erosion, sediment delivery and in-stream transport processes, based on INCA-sed (Jarritt and Lawrence, 2007; Lazar et al., 2010); (2) the separation of total P into particulate and dissolved forms, to better describe P loss and transport mechanisms and potential bioavailability; (3) the adoption of adsorption isotherms to describe the interaction between solid and dissolved P; and (4) removal of the separation of TP into inorganic and organic fractions, primarily motivated by a lack of monitoring data to parameterise the two phases separately. The model was later adapted to allow for the simulation of fully branched river networks (Whitehead et al., 2011). The most recent phase of model development included addressing a number of issues identified by Jackson-Blake et al. (2015). Key improvements included: (1) a reformulation of the equations governing particulate P (PP) delivery to the water course and subsequent in-stream processing, so that PP dynamics are better linked to suspended sediment dynamics, and (2) replacing the constant equilibrium P concentration of zero sorption parameter (EPC_0) with a dynamic variable, calculated as a function of adsorbed P.

In this paper we describe the equations under-pinning INCA-P v1.4.4 (Section 2), providing the first full model description paper since Wade et al. (2002a). We then present a test application to the Tarland Burn catchment, in northeast Scotland (Section 3). This application is used to demonstrate the improved PP simulation and ability to simulate long-term soil P dynamics in the latest version of the model. Finally, we discuss model applicability and limitations (Section 4).

2. Description of INCA-P v1.4.4

2.1 Model overview and conceptual framework

INCA-P operates at a daily time step, tracking the stores and fluxes of water, sediment, dissolved and particulate P in both the land and in-stream phases of a river catchment. The model is spatially 'semi-distributed' (Figure 1): the water course is split into reaches with associated sub-catchments. Two spatial set-ups are possible – the traditional set-up, in which there is a single main stem, or a branched set-up (Whitehead et al., 2011). The branched version allows in-stream processes and effluent inputs in tributaries to be simulated, and can be useful in larger catchments or complex river networks. Each sub-catchment is split into landscape classes, as many as are desired or warranted by the data resolution or needs of the study. Landscape classes are "functional units": within each class, P inputs, plant uptake, soils and flow pathways should be similar, although classes are often based on land use and/or soil type, for convenience. All land-based processes are calculated for a generic 1 km^2 cell for each landscape class within each sub-catchment. Water, sediment, total dissolved P (TDP) and particulate P (PP) outputs from the 1 km^2 cell for each land class are multiplied by the land class area, and summed to provide total inputs from the sub-catchment to the reach. These inputs are assumed to enter the stream reach directly, rather than being routed spatially from one land class to another. Reach inputs are therefore from the land phase and from any upstream reaches.

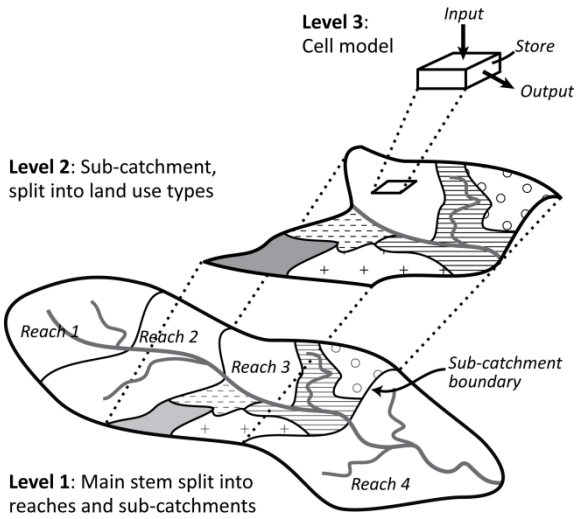

Figure 1: The three-tiered semi-distributed spatial set-up used by INCA. After (Wade et al., 2002a). When using the branched version of the model, tributaries may also be split into reaches with associated sub-catchments.

The main stores, processes and pathways in INCA-P are summarised in Figure 2. The model has six main modules:

1) *Hydrological module*: calculates the flow of water through terrestrial flow paths and the water course. Three terrestrial flow pathways are simulated: quick flow, soil water flow and groundwater flow. Quick flow drives terrestrial erosion and sediment transport to the stream and is primarily conceptualised as

being made up of infiltration and saturation excess overland flow; in practice it is also likely to include drain and ditch flow and preferential flow through soil cracks and macropores. Soil water flow does not affect erosion rates, and travels along slower flow paths than quick flow. Groundwater flow is slower still, sustaining stream flows during baseflow. A more detailed description of the hydrology model and associated equations, variables and parameters is provided in Appendix A;

2) *Sediment module*: based on INCA-sed (Jarritt and Lawrence, 2007; Lazar et al., 2010), which describes erosion, sediment transport to the stream and subsequent entrainment and deposition. Erosion is by splash detachment and flow erosion of bulk sediment, whilst five grain size classes are considered separately for in-stream processes. A full description of the sediment-related processes and equations is provided in Appendix B;

3) *Snow accumulation and melt module* (Appendix C): describes snow depth and snow melt calculations. Snow depth is used in the soil temperature calculations and snow melt may be used in the infiltration equations. Appendix C also describes the soil temperature equation used;

4) *Land phase P module* (Section 2.3): simulates P storage, transformations and fluxes in catchment soils, soil water, quick flow and groundwater;

5) *In-stream P module* (Section 2.4): simulates in-stream P storage, transformations and fluxes;

6) *In-stream biomass*: describes the growth and death of epiphytic algae and macrophytes, which affect in-stream TDP. A full description of the processes and associated equations is provided in Appendix D.

Ordinary differential equations (ODEs) are used to describe the rate of change in volume or mass of model state variables with respect to time. These are all simple mass balance calculations of the form: *change in store* $\propto$ *(input flux – output flux)*. Initial conditions must be provided for each state variable, and these are either user-supplied or calculated within the model; full details are given in Appendix E.

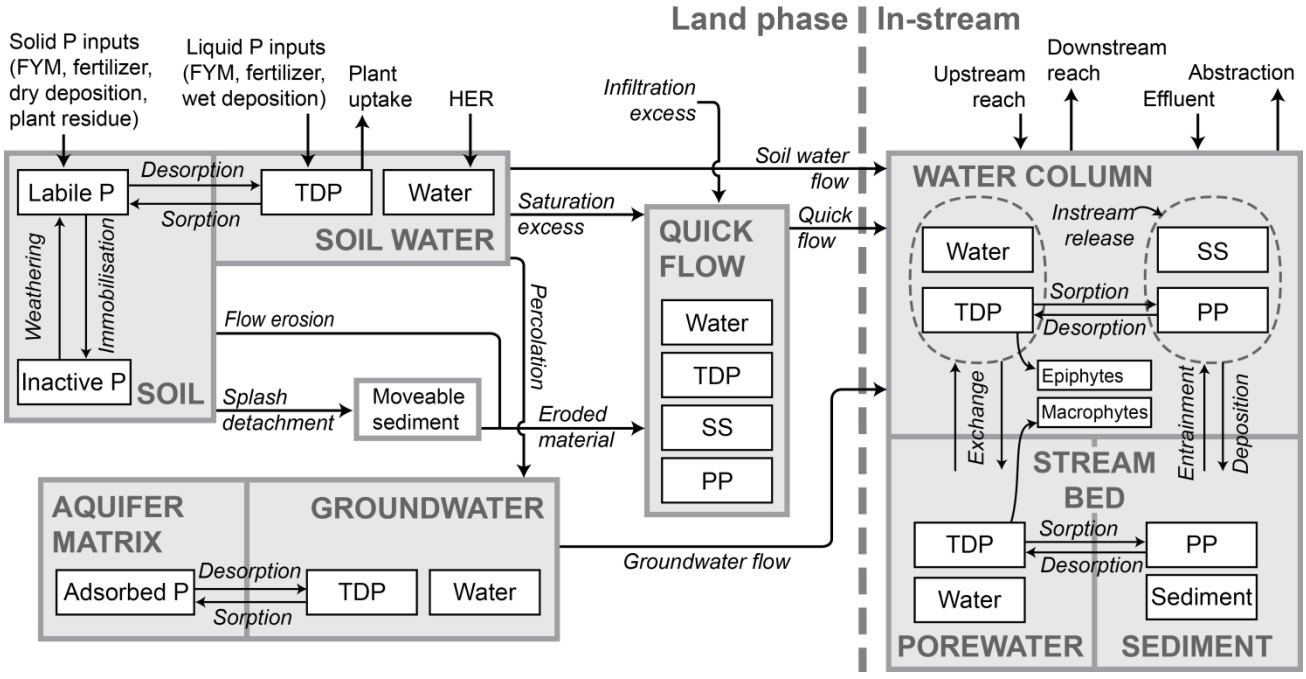

Figure 2: Schematic of the main stores, processes and pathways in INCA-P v1.4.4. Grey boxes show the various compartments simulated. Within these, white boxes show the state variables whose volume (water) or mass (sediment, P

species, in-stream biota) are tracked through the simulation. Arrows show fluxes within and between compartments. P: phosphorus, SS: suspended sediment, TDP: total dissolved P, PP: particulate P, FYM: manure, HER: hydrologically effective rainfall. Modified from Jackson-Blake et al. (2015).

2.2 Data requirements and model outputs

The model requires input daily time series of hydrologically effective rainfall (HER), soil moisture deficit (SMD), precipitation and mean air temperature. HER is the rainfall that contributes to in-stream flow, after accounting for evapotranspiration losses and replenishment of the soil moisture deficit. Where available, multiple hydrological time series can be used to account for spatial variations within a catchment. Both HER and SMD must be generated using an external hydrological model, e.g. PERSiST (Futter et al., 2014), although there are plans for hydrological inputs and soil water levels to be calculated internally in future versions of the model.

Data required for model parameterisation are summarised in Table 1, whilst Appendix F provides a list of user-supplied model parameters, together with an indication of which may be based on data and which must be calibrated. Soil and quick flow equations are land class specific, so associated parameters are specified for each land class. Groundwater equations are sub-catchment specific, to simulate variations in aquifer behaviour in response to larger-scale changes in geology along a river system. Groundwater parameters are therefore specified for each sub-catchment.

A number of datasets are required for robust model calibration. As a minimum, in-stream discharge and water chemistry data are needed, with the exact requirements depending on the complexity of the catchment and the purposes of the model application. If the emphasis is on simulating dissolved P, then in-stream dissolved P concentration data may suffice. If however the aim is to look at total or particulate P, then in-stream suspended sediment data should be available, ideally also PP data. If multiple reaches are simulated, one or both of discharge and water chemistry data should be available for the bottom of each reach. The frequency of the observed data used for model calibration is also very important. In many areas, a large proportion of P transport occurs during flow peaks, which may be missed by low frequency sampling (Cassidy and Jordan, 2011). Unless baseflow P concentrations are the main focus of the modelling study, lower frequency data should therefore be supplemented wherever possible by event sampling, to reduce the risk of obtaining unrealistic model output (Jackson-Blake and Starrfelt, 2015). Finally, to help ensure that the right processes are operating, data to help constrain soil water and groundwater P inputs are highly recommended, such as soil and groundwater TDP concentrations and fluxes, edge-of-field discharge and chemistry data, and data to constrain effluent inputs.

Key data required for model parameterisation	Data required per
Land use and soil types in the sub-catchment, to define landscape classes Annual fertilizer and manure application rates Maximum annual plant P uptake rates Soil properties: total soil P, bulk density	Landscape class
Sub-catchment area Baseflow index Initial groundwater TDP concentration Likely range in soil water TDP concentration (see Section 2.3.1)	Sub-catchment
Paired discharge and stream velocity data (to parameterise Equation A-21) Reach geometry (length, average slope and width) Effluent P inputs (ideally TDP, PP and SS), as a mean flow and concentration or a time series Abstraction rate (mean flow or a time series)	Reach

Table 1: Key datasets required to parameterise INCA-P

Model outputs include: (1) daily and annual land class-specific water, sediment and P fluxes for all processes and stores; (2) daily time series of land class-specific flows and P concentrations in soil water, groundwater and quick flow; (3) daily time series of flows and concentration of TDP, soluble reactive P (SRP), PP, total P (TP) and suspended sediment (SS) in the water column in each reach. SRP is calculated empirically from TDP (Section 2.4.1), and so is not specifically included in Figure 2; and (4) daily time series of macrophyte and epiphytic algae biomass.

2.3 Land phase phosphorus model

Within the model, P is transported from the land phase to the stream via the three flow pathways: soil water flow, groundwater flow and quick flow (Figure 2). All variables in the land phase P equations are defined in Table 2, together with their units and how they are determined. Constants within equations which have not been assigned a variable name are unit conversions (e.g. 86400 s day^{-1}). Within the model code, guards are present to prevent 'divide by zero' errors and to minimize the likelihood of floating point errors; these are not detailed below.

Variable	Description	Units	Source
A_{LU}	Area of landscape class in sub-catchment	%	Input parameter
A_{SC}	Sub-catchment area	km^2	Input parameter
β	Base flow index	-	Input parameter
C_{immob}	Chemical immobilisation factor	day^{-1}	Input parameter
$C_{sat,aquifer}$	P saturation for aquifer matrix	kg P kg sed^{-1}	Input parameter
$C_{sat,labile}$	Maximum soil labile P content	kg P kg sed^{-1}	Input parameter
C_{temp}	Temperature factor	-	Equation 13
C_{uptake}	Plant P uptake factor	m day^{-1}	Input parameter
$C_{weathering}$	Weathering factor	day^{-1}	Input parameter
day_{year}	Day of the year	-	Model calculates
$dP_{sorbed,soil}/dt$	Rate of change in soil P sorption	kg km^{-2} day^{-1}	Equation 5
E_{PP}	PP enrichment factor	-	Input parameter
$EPC_{0,gw}$	Groundwater EPC_0	mg l^{-1}	Equation 17
$EPC_{0,soil}$	Soil EPC_0	mg l^{-1}	Equation 6
F_{period}	Fertilizer addition period	days	Input parameter
F_{start}	Day number when fertilizer addition starts	-	Input parameter
G_{amp}	Plant growth curve amplitude	-	Input parameter
G_{offset}	Plant growth curve vertical offset	-	Input parameter
G_{period}	Growing season length	days	Input parameter
G_{start}	Start of the growing season (day of year)	-	Input parameter
$K_{f,gw}$	Groundwater P sorption coefficient	l kg $soil^{-1}$	Input parameter
$K_{f,soil}$	Soil P sorption coefficient	l kg $soil^{-1}$	Input parameter
K_{gw}	Groundwater sorption scaling factor	day^{-1}	Input parameter
K_{soil}	Soil sorption scaling factor	day^{-1}	Input parameter
$M_{aquifer}$	Aquifer mass	kg km^{-2}	Equation 18
$m_{aquifer,areal}$	Aquifer mass per m^2 (depth × density)	10^3 kg m^{-2}	Input parameter
m_{land}	Reach sediment input per unit area	kg km^{-2} day^{-1}	Equation B-5
$M_{land,total}$	Reach sediment input	kg day^{-1}	Equation B-6
M_{soil}	Soil mass	kg km^{-2}	Equation B-8
n_{gw}	Groundwater Freundlich isotherm constant	-	Input parameter
n_{soil}	Soil Freundlich isotherm constant	-	Input parameter
$P_{dep,solid}$	Annual atmospheric dry P deposition	kg ha^{-1} yr^{-1}	Input parameter/time series
$P_{dep,wet}$	Daily atmospheric wet P deposition	kg ha^{-1} day^{-1}	Equation 4
$P_{dep,wet,annual}$	Annual atmospheric wet P deposition	kg ha^{-1} yr^{-1}	Input parameter/time series
$P_{inactive,soil}$	Inactive P mass in the soil	kg km^{-2}	Equation 11
$P_{labile,soil}$	Labile P mass in the soil	kg km^{-2}	Equation 9
$P_{liq,fert}$	Liquid fertilizer P inputs	kg ha^{-1} day^{-1}	Input parameter/time series
$P_{liq,in}$	Sum of liquid P inputs to the soil	kg ha^{-1} day^{-1}	Equation 3
$P_{liq,manure}$	Liquid manure P inputs	kg ha^{-1} day^{-1}	Input parameter/time series
$P_{maxUptake,day}$	Maximum daily plant P uptake	kg ha^{-1} day^{-1}	Input parameter
$P_{maxUptake,yr}$	Maximum annual plant P uptake	kg ha^{-1} yr^{-1}	Input parameter
$P_{PP,land}$	Reach PP input from the land phase	kg day^{-1}	Equation 21
$P_{residue}$	Plant residue soil P inputs	kg ha^{-1} day^{-1}	Input parameter/time series
$P_{solid,fert}$	Solid fertilizer P inputs	kg ha^{-1} day^{-1}	Input parameter/time series
$P_{solid,in}$	Sum of solid P inputs to the soil	kg ha^{-1} day^{-1}	Equation 10
$P_{solid,manure}$	Solid manure P inputs	kg ha^{-1} day^{-1}	Input parameter/time series
$P_{sorbed,gw}$	P mass in the aquifer matrix	kg km^{-2}	Equation 16
$P_{TDP,gw}$	TDP mass in groundwater	kg km^{-2}	Equation 14
$P_{TDP,land}$	Reach TDP input from the land phase	kg day^{-1}	Equation 22
$P_{TDP,quick}$	TDP mass in quick flow	kg km^{-2}	Equation 19
$P_{TDP,soil}$	TDP mass in soil water	kg km^{-2}	Equation 1
P_{uptake}	Plant uptake of P from the soil water	kg km^{-2} day^{-1}	Equation 7
q_{gw}	Groundwater flow	m^3 s^{-1} km^{-2}	Equation A-13
q_{quick}	Quick flow	m^3 s^{-1} km^{-2}	Equation A-11
$q_{satExcess}$	Saturation excess flow	m^3 s^{-1} km^{-2}	Equation A-8
q_{soil}	Soil water flow	m^3 s^{-1} km^{-2}	Equation A-5
$q_{soil\ out}$	Soil water flow and saturation excess	m^3 s^{-1} km^{-2}	Equation A-3
R_{eff}	Hydrologically effective precipitation flux	m^3 s^{-1} km^{-2}	Equation A-1
S_{PGI}	Seasonal plant growth index	-	Equation 8
S_{SMD}	Soil moisture factor	-	Equation 12
SMD	Soil moisture deficit	mm	Input time series
SMD_{max}	Maximum soil moisture deficit	mm	Input parameter
T_{air}	Air temperature	°C	Input time series
$T_{immob,0}$	Lower temperature threshold for immobilisation	°C	Input parameter
t_{Q10}	Change in rate with a 10°C change in temperature	-	Input parameter
$t_{Q10,base}$	Temperature at which the rate response is 1	°C	Input parameter
T_{soil}	Soil temperature	°C	Equation C-6
TDP_{gw}	Groundwater TDP concentration	mg l^{-1}	Equation 15

Variable	Description	Units	Source
TDP_{quick}	Quick flow TDP concentration	mg l^{-1}	Equation 20
$TDP_{soilwater}$	Soil water TDP concentration	mg l^{-1}	Equation 2
V_{gw}	Groundwater volume	m^3 km^{-2}	Equation A-14
V_{quick}	Quick flow volume	m^3 km^{-2}	Equation A-12
$V_{soilwater}$	Soil water volume	m^3 km^{-2}	Equation A-7

Table 2: Variables and parameters in terrestrial process equations. Units of '-': dimensionless. Equation numbers preceded by a letter are in the Appendices.

2.3.1 Soil processes

The soil compartment is composed of soil water, which contains dissolved P as TDP, and the soil matrix, which contains P adsorbed to or fixed in soil particles (Figure 2). This soil compartment is assumed to broadly equate to the soil O/A horizon or the plough layer (if present).

a) Dissolved phosphorus

The rate of change in soil water TDP mass with time is given by Equation 1 and the associated soil water TDP concentration by Equation 2. Phosphorus inputs to the soil water include any liquid inputs, usually primarily from inorganic fertilizer and manure (Equation 3) but also potentially from wet atmospheric deposition (Equation 4) and any P desorbed from the soil matrix (Equation 5).

Equation 1: Change in mass of TDP in the soil water, $P_{TDP,soil}$, with time (kg km^{-2} day^{-1}). Superscript *t* is the current time step, *t-1* the previous time step

If $V_{soilwater} > 0$: $\frac{dP_{TDP,soil}}{dt} = 100P_{liq,in} - \frac{dP_{sorbed,soil}}{dt} - P_{uptake} - \frac{86400\ q_{soil\_out}P_{TDP,soil}}{V_{soilwater}}$

Otherwise: $\frac{dP_{TDP,soil}}{dt} = 100P_{liq,in} - \frac{dP_{sorbed,soil}}{dt} - P_{uptake}$

If $\frac{P_{labile,soil}}{M_{soil}} \geq C_{sat,labile}$: $P^{t}_{TDP,soil} = P^{t-1}_{TDP,soil} + (P_{labile,soil} - C_{sat,labile}M_{soil})$

Equation 2: Soil water TDP concentration, $TDP_{soilwater}$ (mg l^{-1})

$$TDP_{soilwater} = 10^3 \frac{P_{TDP,soil}}{V_{soilwater}}$$

Equation 3: Liquid P inputs to the soil water, $P_{liq,in}$ (kg ha^{-1} day^{-1})

If day_{year} is in the range $(F_{start}, F_{start} + F_{period})$: $P_{liq,in} = P_{liq,manure} + P_{liq,fert} + P_{dep,wet}$

Otherwise: $P_{liq,in} = P_{dep,wet}$

Equation 4: Wet deposition to the soil water, $P_{dep,wet}$ (kg ha^{-1} day^{-1}), where subscript *d* is the Julian day

$$P_{dep,wet} = \frac{R_{eff}}{\sum_{day=1}^{day_{year}} R_{eff,d}} P_{dep,wet,annual}$$

The change in mass of P adsorbed to or desorbed from the soil (Equation 5) is calculated using a form of the Freundlich isotherm (House and Denison, 2000), where the change in mass adsorbed is proportional to the difference between the soil water TDP concentration and the equilibrium TDP concentration at which no

adsorption or desorption occurs ($EPC_{0,soil}$). In earlier versions of the model $EPC_{0,soil}$ was a constant user-supplied parameter, but it is now a dynamic variable, dependent on the mass of P in the labile soil store (Equation 6). This allows for the simulation of longer term soil P dynamics and fits with monitoring data showing $EPC_{0,soil}$ increasing as soil P enrichment increases (e.g. Lin and Banin, 2005).

Equation 5: Change in mass of P sorbed as labile soil P with time, $dP_{sorbed,soil}/dt$ (kg km^{-2} day^{-1})

$$\frac{dP_{sorbed,soil}}{dt} = 10^{-3} K_{soil} \left(TDP_{soilwater}^{\frac{1}{n_{soil}}} - EPC_{0,soil}^{\frac{1}{n_{soil}}} \right) V_{soilwater}$$

Equation 6: The soil equilibrium TDP concentration of zero sorption, $EPC_{0,soil}$ (mg l^{-1})

If $M_{soil} > 0$ and $P_{labile,soil} > 0$ and $K_{f,soil} > 0$: $EPC_{0,soil} = \left(\frac{10^6}{K_{f,soil}} \frac{P_{labile,soil}}{M_{soil}} \right)^{n_{soil}}$

Otherwise: $EPC_{0,soil} = TDP_{soilwater}$

The Freundlich isotherm parameters $K_{f,soil}$ and n_{soil} are measurable, but it is a time-consuming process and in practice data for a given study area are rarely available, particularly given that parameter values are needed on a soil-by-soil basis, as adsorption depends on soil Fe and Al oxyhydroxide content, organic matter content, etc. There are also issues with the transferability of lab measurements to field situations, as shaking in the lab results in an overestimation of reaction rates, without taking into account the effects of high concentrations and redox conditions in pore waters (House and Denison, 2002; Stutter et al., 2010). Perhaps more importantly, model processes reflect an averaged response of both organic and inorganic transfers happening in reality. These parameters are therefore usually calibrated, ideally informed by measured soil water TDP concentration and labile P content across a gradient of values for a given soil type (e.g. Section 3.2.3, point 6), and may have little physical meaning.

TDP outputs from the soil water are via plant uptake (Equation 7), adsorption (Equation 5) and soil water drainage (the final term in Equation 1). Plant uptake is limited so that it cannot exceed user-supplied maximum daily or annual values (Equation 7), and varies seasonally (Equation 8). Finally, if the labile soil P content has reached an optional user-specified P saturation threshold, any additional inputs to the labile P store are converted to soil water TDP (second part of Equation 1).

Equation 7: Plant uptake of P from the soil water, P_{uptake} (kg km^{-2} day^{-1})

If day_{year} is outside the range G_{start}: $(G_{start} + G_{period})$ or if $P_{up,cumulative} > P_{maxUptake,yr}$, then $P_{uptake} = 0$

(where $P_{up,cumulative}$ (kg ha^{-1}) $= \frac{1}{100} \sum_{day=1}^{current\ day} P_{uptake}$)

Otherwise, $P_{uptake} = \text{minimum}\{10^6 C_{uptake} C_{temp} S_{SMD} S_{PGI} \frac{P_{TDP,soil}}{V_{soilwater}}, 100 P_{maxUptake,day}\}$

Equation 8: Seasonal plant growth index, S_{PGI}

$$S_{PGI} = G_{offset} + G_{amp} \sin\left(\frac{2\pi}{365} (day_{year} - G_{start}) \right)$$

b) Soil phosphorus

Phosphorus in the soil is split into a 'labile' store of water-soluble P, which can take part in sorption reactions, and an 'inactive' store of insoluble P (e.g. inactive mineral P or recalcitrant organic material), which does not (Figure 2). The rate of change in labile soil P mass over time is given by Equation 9. Inputs include solid P inputs, usually primarily from fertilizer and manure (Equation 10), any P adsorption from the soil water (Equation 5) and breakdown of inactive soil P (e.g. by chemical weathering or mineralization of stable phases). Outputs are via erosion and immobilisation in inactive soil P. The resulting soil labile P mass may be limited by P saturation (Equation 9).

Equation 9: Change in mass of labile soil P, $P_{labile,soil}$, with time (kg km^{-2} day^{-1})

$$\frac{dP_{labile,soil}}{dt} = 100P_{solid,in} + \frac{dP_{sorbed,soil}}{dt} + C_{weathering}C_{temp}P_{inactive,soil} - m_{land}\frac{P_{labile,soil}}{M_{soil}} - C_{immob}C_{temp}P_{labile,soil}$$

If $\frac{P_{labile,soil}}{M_{soil}} \geq C_{sat,labile}$: $P_{labile,soil} = C_{sat,labile}M_{soil}$

Equation 10: Solid P inputs to the soil, $P_{solid,in}$ (kg ha^{-1} day^{-1})

If day_{year} in range $(F_{start}: F_{start} + F_{period})$: $P_{solid,in} = P_{solid,manure} + P_{solid,fert} + P_{residue} + \frac{P_{dep,solid}}{365}$

Otherwise: $P_{solid,in} = P_{residue} + \frac{P_{dep,solid}}{365}$

The inactive store represents firmly-bound P, so the only inputs are from immobilisation of labile soil P and outputs are through erosion and weathering (Equation 11).

Equation 11: Change in the mass of inactive soil P, $P_{inactive,soil}$, with time (kg km^{-2} day^{-1})

$$\frac{dP_{inactive,soil}}{dt} = C_{immob}C_{temp}P_{inactive,soil} - m_{land}\frac{P_{inactive,soil}}{M_{soil}} - C_{weathering}C_{temp}P_{labile,soil}$$

This representation of soil P processes is highly simplified. In reality, soil P is present in a continuum of interlinked organic and inorganic states of varying extractability, hysteresis effects are common in P transfers between the states, and organic and inorganic soil P fractions are affected by different processes. However, the understanding of how detailed soil chemical and biological processes upscale to the catchment-scale is arguably not yet advanced enough to be usefully incorporated into a catchment-scale model, and there is certainly a lack of data to constrain such processes at a catchment scale. Although these simplifications reduce the input data requirements, they make it difficult to base initial soil P mass in the two stores on measured data, such as soil test P data. Instead, an estimate of total P data is needed, which is less commonly available (Section 3.2.3).

c) Reaction rates: moisture and temperature dependency

A number of reaction rates are dependent on soil moisture and temperature. The soil moisture factor in Equation 7 results in slower plant uptake of P in drier soils, tending to zero as the SMD approaches a maximum value such as the permanent wilting point (Equation 12). The temperature factor in Equations 7, 9 and 11 is based on a Q_{10} temperature coefficient, i.e. the rate of change as a consequence of increasing the

temperature by 10°C, with faster uptake, immobilisation and weathering at higher temperatures (Equation 13). The temperature factor calculation requires a time series of soil temperature, which is calculated from air temperature using a model developed by Rankinen et al. (2004a), taking the insulating effect of snow cover into account (Appendix C, Equation C-6).

Equation 12: Soil moisture factor, S_{SMD}

$$S_{SMD} = \frac{SMD_{max} - SMD}{SMD_{max}}$$

Equation 13: Temperature factor, C_{temp}

For plant uptake and chemical weathering: $C_{temp} = t_{Q10}^{\frac{T_{soil} - t_{Q10,base}}{10}}$

For chemical immobilisation: If $T_{air} > T_{immob,0}$: $C_{temp} = t_{Q10}^{\frac{T_{soil} - t_{Q10,base}}{10}}$, otherwise $C_{temp} = 0$

Although daily plant uptake varies with temperature and soil moisture, the daily or annual maximum uptake values are constant user-supplied parameters, and therefore do not vary according to climatic conditions. A potential future improvement would be for these additional parameters to also be climate-dependent, to help simulate e.g. the greater crop yield and therefore P uptake that might be expected in some areas under a warmer, wetter climate.

2.3.2 Groundwater processes

Groundwater is considered to be water in the soil B/C horizons or deeper. Phosphorus processes in the groundwater compartment are similar conceptually to the soil compartment, with a water volume with associated TDP and a solid P store in the aquifer matrix (Figure 2). The rate of change in the mass of TDP in the groundwater with time is given by Equation 14 and the groundwater TDP concentration by Equation 15. TDP inputs to the groundwater are via percolation of soil water and any desorption from the aquifer matrix (Equation 16); outputs are via adsorption (Equation 16) and drainage to the stream. As in the soil, $EPC_{0,gw}$ is dynamic, dependent on the mass of P in the aquifer matrix (Equation 17). Estimating this requires an estimate of the sediment mass in the aquifer involved in P exchange reactions (Equation 18).

Equation 14: Change in groundwater TDP mass, $P_{TDP,gw}$, with time (kg km^{-2} day^{-1}), where superscript *t* is the current time step, *t-1* the previous time step

$$\frac{dP_{TDP,gw}}{dt} = \frac{86400\ \beta q_{soil} P_{TDP,soil}}{V_{soilwater}} - \frac{dP_{sorbed,gw}}{dt} - \frac{86400\ q_{gw} P_{TDP,gw}}{V_{gw}}$$

If $\frac{P_{sorbed,gw}}{M_{aquifer}} \geq C_{sat,aquifer}$: $P_{TDP,gw}^{t} = P_{TDP,gw}^{t-1} + (P_{sorbed,gw} - C_{sat,aquifer} M_{aquifer})$

Equation 15: Groundwater TDP concentration, TDP_{gw} (mg l^{-1})

$$TDP_{gw} = 10^3 \frac{P_{TDP,gw}}{V_{gw}}$$

Equation 16: Change in mass of P sorbed in the groundwater, $P_{sorbed,gw}$, with time (kg km^{-2} day^{-1})

$$\frac{dP_{sorbed,gw}}{dt} = 10^{-3} K_{gw} \left(TDP_{gw}^{\frac{1}{n_{gw}}} - EPC_{0,gw}^{\frac{1}{n_{gw}}} \right) V_{gw}$$

$$\text{If } \frac{P_{sorbed,gw}}{M_{aquifer}} \geq C_{sat,aquifer}: P_{sorbed,gw} = C_{sat,aquifer} M_{aquifer}$$

Equation 17: The groundwater equilibrium P concentration of zero sorption, $EPC_{0,gw}$ (mg l^{-1})

$$\text{If } P_{sorbed,gw} > 0 \text{ and } K_{f,gw} > 0: EPC_{0,gw} = \left(\frac{10^6}{K_{f,gw}} \frac{P_{sorbed,gw}}{M_{aquifer}} \right)^{n_{gw}}$$

$$\text{Else: } EPC_{0,gw} = TDP_{gw}$$

Equation 18: Aquifer mass involved in P sorption reactions, $M_{aquifer}$ (kg km^{-2})

$$M_{aquifer} = 10^9 m_{aquifer,areal}$$

Including adsorption processes in the groundwater compartment in theory allows legacy groundwater P to be simulated, for example due to historic prolonged inputs to groundwater from sewage effluent or septic tanks. However, in practice the parameterisation of these equations requires more detailed knowledge of groundwater and aquifer geometry, P content and sorption characteristics than is available in many areas. There are also questions as to how representative these equations can be of groundwater P processes, as the influence of the wider geochemical environment on P mobility is not taken into account (discussed further in Section 4).

2.3.3 Quick flow processes

Water, sediment and dissolved and particulate P are stored in the quick flow compartment and transported to the watercourse via quick flow (Figure 2). Unlike in the soil compartment, no transformations between dissolved and particulate P are included in the model.

The rate of change in mass of TDP stored in the quick flow compartment is given by Equation 19 and the quick flow TDP concentration by Equation 20. Inputs are from saturation excess flow, and the simplifying assumption is made that saturation excess flow has the same TDP concentration as soil water; outputs are via runoff to the stream. Infiltration excess flow only provides an input of water to quick flow, not of P, and is therefore not included in Equation 19. Infiltration excess events may therefore result in a dilution of quick flow TDP concentrations, as they cause an increase in quick flow water volume.

Equation 19: Change in mass of TDP in quick flow, $P_{TDP,quick}$, with time (kg km^{-2} day^{-1})

$$\frac{dP_{TDP,quick}}{dt} = 86400 \left(\frac{q_{satExcess} P_{TDP,soil}}{V_{soilwater}} - \frac{q_{quick} P_{TDP,quick}}{V_{quick}} \right)$$

Equation 20: TDP concentration in quick flow, TDP_{quick} (mg l^{-1})

$$TDP_{quick} = 10^3 \frac{P_{TDP,quick}}{V_{quick}}$$

Particulate P is only transported to the stream via quick flow, and the PP mass transported is linearly related to the mass of soil transported. For a full description of the terrestrial sediment equations see Appendix B.1; in short, simulated erosion occurs via splash detachment and flow erosion, and sediment yield to the stream is dependent on the transport capacity of quick flow. Eroded material is frequently enriched in P relative to parent soils due to the selective transport of finer-grained, P-rich particles (Sharpley, 1980). To take this into account, there is the option to include an enrichment factor, E_{PP}, in Equation 21. In reality, P enrichment decreases as the size of the rainfall event increases, and so the simple constant, user-supplied enrichment factor should be considered a longer-term average.

Equation 21: Reach PP input from the land phase, $P_{PP,land}$ (kg day^{-1}), where superscript j denotes the landscape class and $P^{j}_{PP,land}$ is the flux per km^2

$$P^{j}_{PP,land} = E_{PP} M_{land,total} \frac{\left(P_{labile,soil} + P_{inactive,soil}\right)}{M_{soil}}$$

$$P_{PP,land} = \sum_{land\ use\ class\ j=1}^{n\ land\ use\ classes} A_{SC} \frac{A^{j}_{LU}}{100} P^{j}_{PP,land}$$

A number of potentially important inputs to quick flow TDP and PP, such as runoff from farm yards or washoff of freshly-applied fertilizers or manures, are not explicitly accounted for in the model (discussed further in Section 4).

2.3.4 Inputs from the land phase to the stream

Inputs of TDP from the terrestrial compartment to the stream are calculated by summing the contributions from soil water flow, quick flow and groundwater flow, taking into account how these vary between land classes and sub-catchments (Equation 22). As PP only enters the stream via quick flow, the PP input to the stream is equivalent to Equation 21.

Equation 22: Reach TDP input from the land phase, $P_{TDP,land}$ (kg day^{-1}), where superscript j denotes the landscape class

$$\frac{dP^{j}_{TDP,land}}{dt} = 86400 \left(\frac{q_{soil} P_{TDP,soil}}{V_{soilwater}} + \frac{q_{gw} P_{TDP,gw}}{V_{gw}} + \frac{q_{quick} P_{TDP,quick}}{V_{quick}} \right)$$

$$P_{TDP,land} = \sum_{land\ use\ class\ j=1}^{n\ land\ use\ classes} A_{SC} \left(\frac{A^{j}_{LU}}{100} \right) P^{j}_{TDP,land}$$

2.4 In-stream phosphorus model

In-stream, water column and stream bed processes are simulated separately (Figure 2). In the water column, P may be present as TDP or PP, whilst P in the stream bed is present as TDP within porewaters and as PP in bed sediments. TDP exchange between the water column and the stream bed occurs via porewater flushing, whilst PP exchange occurs via particle deposition and resuspension.

In-stream equations described below are solved for each reach; all variables are defined in Table 3. Guards are present in the code to prevent 'divide by zero' errors and to minimize the likelihood of floating point errors; these are not detailed below.

Variable	Description	Units	Source
$B_{growth,epi}$	Growth of epiphyte biomass	g C m^{-2} day^{-1}	Equation D-2
$B_{growth,mac}$	Growth of macrophyte biomass	g C m^{-2} day^{-1}	Equation D-5
$C_{P,epi}$	Proportion of P in epiphytes	g P g C^{-1}	Input parameter
$C_{P,mac}$	Proportion of P in macrophytes	g P g C^{-1}	Input parameter
$C_{sat,bed}$	Maximum P:sed ratio in the stream bed	kg P kg sed^{-1}	Input parameter
$C_{sat,wc}$	Maximum P:sed ratio in suspended material	kg P kg sed^{-1}	Input parameter
c_{SRP}	Regression between TDP and SRP (y-intercept)	mg l^{-1}	Input parameter
d_{bed}	Bed sediment depth	m	Input parameter
$dP_{sorbed,bed}/dt$	Change in mass of P adsorbed in the stream bed	kg day-1	Equation 32
$dP_{sorbed,wc}/dt$	Change in mass of P adsorbed to suspended sediment	kg day-1	Equation 27
DOC_{wc}	Mean water column DOC concentration	mg l^{-1}	Input parameter
$E_{pw,wc}$	Fraction exchanged (water column and stream bed)	day^{-1}	Input parameter
$EPC_{0,pw}$	Stream bed porewater EPC_0	mg l^{-1}	Equation 33
$EPC_{0,wc}$	Water column EPC_0	mg l^{-1}	Equation 29
$K_{f,pw}$	Porewater sorption coefficient	l kg sed^{-1}	Input parameter
$K_{f,wc}$	Water column sorption coefficient	l kg $soil^{-1}$	Input parameter
K_{pw}	Stream bed porewater sorption scaling factor	day^{-1}	Input parameter
K_{wc}	Water column sorption scaling factor	day^{-1}	Input parameter
L_{reach}	Reach length	m	Input parameter
M_{bed}	Reach bed sediment mass	kg	Equation B-24
m_{dep}	Mass of sediment deposited on the stream bed	kg m^{-2} day^{-1}	Equation B-20
m_{DOC}	Ratio of dissolved hydrolysable P to DOC	-	Input parameter
m_{ent}	Mass of sediment entrained from the stream bed	kg m^{-2} day^{-1}	Equation B-14
m_{SRP}	Regression between TDP and SRP (gradient)	-	Input parameter
M_{SS}	Reach suspended sediment mass	kg	Equation B-9
n_{pw}	Porewater Freundlich isotherm constant	-	Input parameter
n_{wc}	Water column Freundlich isotherm constant	-	Input parameter
$P_{PP,bed}$	PP mass in the stream bed	kg	Equation 42
$P_{PP,dep}$	PP mass deposited to the stream bed	kg day^{-1}	Equation 40
$P_{PP,DS}$	PP output from the bottom of the reach	kg day^{-1}	Equation 41
$P_{PP,ent}$	PP mass entrained from the stream bed	kg day^{-1}	Equation 39
$P_{PP,land}$	PP output from the terrestrial compartment	kg day^{-1}	Equation 21
$P_{PP,US}$	PP input from the upstream reach	kg day^{-1}	Model calculates
$P_{PP,wc}$	PP mass in the water column	kg	Equation 37
$P_{TDP,DS}$	TDP output downstream from reach	kg day^{-1}	Equation 26
$P_{TDP,exchange}$	TDP exchange (water column and stream bed)	kg day^{-1}	Equation 28
$P_{TDP,land}$	Reach TDP input from the land phase	kg day^{-1}	Equation 22
$P_{TDP,pw}$	TDP mass in the stream bed porewaters	kg	Equation 31
$P_{TDP,US}$	TDP input from the upstream reach	kg day^{-1}	Model calculates
$P_{TDP,wc}$	TDP mass in the water column	kg	Equation 23
$P_{up,epi}$	TDP uptake by epiphytes	kg day^{-1}	Equation 25
$P_{up,mac}$	TDP uptake by macrophytes	kg day^{-1}	Equation 34
PP_{eff}	Effluent PP concentration	mg l^{-1}	Input parameter/time series
PP_{wc}	Water column PP concentration	mg l^{-1}	Equation 38
q_{abs}	Abstraction rate	m^3 s^{-1}	Input parameter
q_{eff}	Effluent discharge	m^3 s^{-1}	Input parameter/time series
$q_{reach,out}$	Reach outflow	m^3 s^{-1}	Equation A-18
SRP_{wc}	In-stream SRP concentration	mg l^{-1}	Equation 30
TDP_{eff}	Effluent TDP concentration	mg l^{-1}	Input parameter/time series
TDP_{pw}	Stream bed porewater TDP concentration	mg l^{-1}	Equation 35
TDP_{wc}	Water column TDP concentration	mg l^{-1}	Equation 24
θ_{bed}	Bed sediment porosity	-	Input parameter
V_{pw}	Porewater volume	m^3	Equation 36
V_{reach}	Reach water volume	m^3	Equation A-19
w_{reach}	Average reach width	m	Input parameter

Table 3: Variables and parameters in in-stream P equations (units '-' are dimensionless)

2.4.1 Dissolved phosphorus in the water column

The rate of change in water column TDP mass with time is given by Equation 23 and the TDP concentration by Equation 24. Reach TDP inputs are from upstream reaches, the land phase (Equation 22) and sewage effluent. Outputs are via abstractions, uptake by epiphytic algae (Equation 25) and reach outflow (Equation 26). TDP uptake depends on the epiphyte growth rate; the equations underpinning this are given in Appendix D and a description of the underlying scientific basis is provided in Wade et al. (2002a). Sorption reactions in the water column can act as a source or a sink of TDP (Equation 27), as can exchange with stream bed sediments (Equation 28). P saturation of suspended matter may result in additional dissolved P inputs to the water column (second expression in Equation 23).

Equation 23: Change in mass of TDP in the water column, $P_{TDP,wc}$, with time (kg day^{-1}), where superscript *t* is the current time step, *t-1* the previous time step

$$\frac{dP_{TDP,wc}}{dt} = P_{TDP,US} + P_{TDP,land} + 86.4\ TDP_{eff}\, q_{eff} + P_{TDP,exchange} - 86.4\ TDP_{wc}\, q_{abs} - P_{up,epi} - P_{TDP,\mathrm{DS}} - \frac{dP_{sorbed,wc}}{dt}$$

$$If\ \frac{P_{PP,wc}}{M_{SS}} \geq C_{sat,wc}\colon P^{t}_{TDP,wc} = P^{t-1}_{TDP,wc} + (P_{PP,wc} - C_{sat,wc} M_{SS})$$

Equation 24: TDP concentration in the water column, TDP_{wc} (mg l^{-1})

$$TDP_{wc} = 10^{3}\,\frac{P_{TDP,wc}}{V_{reach}}$$

Equation 25: Reach TDP uptake by epiphytic algae, $P_{up,epi}$ (kg day^{-1}):

$$P_{up,epi} = 10^{-3} C_{P,epi} B_{growth,epi} L_{reach} w_{reach}$$

Equation 26: Reach TDP output from the bottom of a reach to the downstream reach, $P_{TDP,DS}$ (kg day^{-1})

$$P_{TDP,DS} = 86400\ \frac{P_{TDP,wc}\, q_{reach,out}}{V_{reach}}$$

Equation 27: Change in mass of P adsorbed to suspended sediments in the water column with time, $dP_{sorbed,wc}/dt$ (kg day^{-1})

$$\frac{dP_{sorbed,wc}}{dt} = 10^{-3} K_{wc} \left(TDP_{wc}^{\frac{1}{n_{wc}}} - EPC_{0,wc}^{\frac{1}{n_{wc}}} \right) V_{reach}$$

Equation 28: In-stream TDP exchange between the water column and stream bed pore waters, $P_{TDP,exchange}$ (kg day^{-1}), in terms of net input to the water column from porewaters

$$P_{TDP,exchange} = 10^{-3} E_{pw,wc} V_{reach} \left(TDP_{pw} - TDP_{wc} \right)$$

As in the land phase, the change in mass of water column adsorbed P during a given time step (Equation 27) depends on the difference between the water column TDP concentration and the water column EPC_0 ($EPC_{0,wc}$). In the latest version of the model $EPC_{0,wc}$ is a dynamic variable dependent on the PP:SS ratio in the water column (Equation 29).

Equation 29: The water column equilibrium P concentration of zero sorption, $EPC_{0,wc}$ (mg l^{-1})

If $M_{SS} > 0$ and $P_{PP,wc} > 0$ and $K_{f,wc} > 0$: $EPC_{0,wc} = \left(\frac{10^6}{K_{f,wc}} \frac{P_{PP,wc}}{M_{SS}}\right)^{n_{wc}}$

Otherwise: $EPC_{0,wc} = TDP_{wc}$

Finally, SRP concentration is calculated from TDP (Equation 30). This calculation can be done in two ways: (a) by assuming a linear relationship with TDP, or (b) by using observed average DOC concentration as a proxy for dissolved hydrolysable P (DHP) and assuming that SRP = TDP – DHP. Either option is a simplification, as the relationship with TDP is likely to vary in space and time and for different P sources. Data from Scottish rivers (Anderson et al., 2010) and the River Kennet (UK) suggest it is broadly appropriate, but this is an area for potential future improvement given that P standards for flowing waters are commonly defined in terms of SRP, which is generally more bioavailable than TDP.

Equation 30: In-stream SRP concentration, SRP_{wc} (mg l^{-1})

Option 1: $SRP_{wc} = m_{SRP}\, TDP_{wc} + c_{SRP}$
Option 2: $SRP_{wc} = TDP_{wc} - m_{DOC}\, DOC_{wc}$

2.4.2 Dissolved phosphorus in the stream bed

Within the stream bed, the rate of change in porewater TDP mass with time is given by Equation 31. TDP exchange with the overlying water column can act as a source or a sink of porewater TDP (Equation 28), as can P sorption reactions (Equation 32). P sorption is calculated using a dynamic EPC_0 (Equation 33), to allow the influence of legacy bed sediment P to be explored, e.g. down-stream of sewage treatment works (Jarvie et al., 2012). Uptake by macrophytes may be an additional TDP output from the stream bed (Equation 34), and depends on the macrophyte growth rate (Appendix D).

Equation 31: Change in mass of TDP in the stream bed porewaters, $P_{TDP,p}$, with time (kg day^{-1}), where superscript *t* is the current time step and *t-1* is the previous time step

$$\frac{dP_{TDP,pw}}{dt} = -P_{TDP,exchange} - \frac{dP_{sorbed,bed}}{dt} - P_{up,mac}$$

If $\frac{P_{PP,bed}}{M_{bed}} \geq C_{sat,bed}$: $P^t_{TDP,pw} = P^{t-1}_{TDP,pw} + (P_{PP,bed} - C_{sat,bed} M_{bed})$

Equation 32: Change in mass of P adsorbed to stream bed sediments with time, $dP_{sorbed,bed}/dt$ (kg day^{-1})

$$\frac{dP_{sorbed,bed}}{dt} = 10^{-3} K_{pw} \left(TDP_{pw}^{\frac{1}{n_{pw}}} - EPC_{0,pw}^{\frac{1}{n_{pw}}}\right) V_{reach}$$

Equation 33: The stream bed equilibrium P concentration of zero sorption, $EPC_{0,pw}$ (mg l^{-1})

If $M_{bed} > 0$ and $P_{PP,bed} > 0$ and $K_{f,pw} > 0$: $EPC_{0,pw} = \left(\frac{10^6}{K_{f,pw}} \frac{P_{PP,bed}}{M_{bed}}\right)^{n_{pw}}$

Otherwise: $\mathrm{EPC_{0,pw}} = TDP_{pw}$

Equation 34: Macrophyte TDP uptake from porewaters, $P_{up,mac}$ (kg day^{-1})

$$P_{up,mac} = 10^{-3} C_{P,mac} B_{growth,mac} L_{reach} w_{reach}$$

Porewater TDP concentration (Equation 35) is calculated assuming that porewater volume is constant over time in each reach (Equation 36).

Equation 35: Porewater TDP concentration, TDP_{pw} (mg l^{-1})

$$TDP_{pw} = 10^{3} \frac{P_{TDP,pw}}{V_{pw}}$$

Equation 36: Porewater volume, V_{pw} (m^3):

$$V_{pw} = w_{reach}\, L_{reach}\, d_{bed}\, \theta_{bed}$$

2.4.3 In-stream particulate phosphorus processes

The rate of change in water column PP mass with time is given by Equation 37 and the PP concentration by Equation 38. PP inputs to the water column are from any upstream reaches, the land phase (Equation 21), sewage effluent and entrainment of stream bed PP (Equation 39). Outputs are via particle settling and deposition (Equation 40), abstraction and outflow from the bottom of the reach (Equation 41). The change in mass of P adsorbed to SS in the water column (Equation 27) may act as an input or an output of PP, and P saturation of suspended matter may limit the water column PP mass (second expression in Equation 37). PP entrainment and settling rates are dependent on SS dynamics, which are described fully in Appendix B.2.

Equation 37: Change in mass of PP in the water column, $P_{PP,wc}$, with time (kg day^{-1})

$$\frac{dP_{PP,wc}}{dt} = P_{PP,US} + P_{PP,land} + 86.4\, PP_{eff}\, q_{eff} + \frac{dP_{sorbed,wc}}{dt} + P_{PP,ent} - P_{PP,dep} - 86.4\, PP_{wc}\, q_{abs} - P_{PP,\mathrm{DS}}$$

If $\frac{P_{PP,wc}}{M_{SS}} \geq C_{sat,wc}$: $P_{PP,wc} = C_{sat,wc} M_{SS}$

Equation 38: Water column PP concentration, PP_{wc} (mg l^{-1})

$$PP_{wc} = 10^{3} \frac{P_{PP,wc}}{V_{reach}}$$

Equation 39: Mass of PP entrained from the stream bed, $P_{PP,ent}$ (kg day^{-1})

If $M_{bed} > 0$: $P_{PP,ent} = m_{ent} \frac{P_{PP,bed}}{M_{bed}} L_{reach} w_{reach}$; otherwise: $P_{PP,ent} = 0$

Equation 40: Mass of PP deposited on the stream bed, $P_{PP,dep}$ (kg day^{-1})

If $M_{SS} > 0$: $P_{PP,dep} = m_{dep} \frac{P_{PP,wc}}{M_{sus}} L_{reach} w_{reach}$; otherwise: $P_{PP,dep} = 0$

Equation 41: Reach PP output downstream, $P_{PP,DS}$ (kg day^{-1})

$$P_{PP,DS} = \frac{86400\ P_{PP,wc}\ q_{reach,out}}{V_{Reach}}$$

The rate of change in stream bed PP mass with time is given by Equation 42. PP may be lost through entrainment (Equation 39) or gained through deposition (Equation 40), whilst P sorption may result in either a loss or a gain (Equation 32). As in the water column, stream bed sediments may become P saturated, in which case additional P is assumed to enter porewater as dissolved P (Equation 31).

Equation 42: Change in mass of PP in the stream bed, $P_{PP,bed}$, with time (kg day^{-1})

$$\frac{dP_{PP,bed}}{dt} = \frac{dP_{sorpbed,bed}}{dt} + P_{PP,dep} - P_{PP,ent}$$

If $\frac{P_{PP,bed}}{M_{bed}} \geq C_{sat,bed}$: $P_{PP,bed} = C_{sat,bed} M_{bed}$

2.5 Technical details and model availability

INCA-P is a 32-bit Microsoft Windows application written in C++. It is available as a command-line version (1.27 MB) or with a graphical user interface (3.75 MB), and will run on Windows XP onwards. The RAM required during simulation depends on the application set-up (number of reaches and landscape units) and application period (number of time steps). A simple one year, single reach set-up requires 6.6 MB of RAM.

The in-stream suspended sediment ODEs are solved using the Backward Differentiation Formula method of CVODE (Cohen and Hindmarsh, 1996); all other ODEs are solved using a 4th order Runge-Kutta-Merson method (Wambecq, 1978). Although this is an adaptive solver, it is not particularly well-suited to solving stiff ODE systems, and is therefore an area for future improvement.

At the time of writing, INCA-P is freely available for non-commercial use and can be obtained under licence for commercial applications. The executable can be requested from the Norwegian Institute for Water Research (NIVA) at www.niva.no/inca/inca-phosphorus (last accessed May 2016).

3. Case study: model application to the Tarland Burn, northeast Scotland

3.1 Introduction to the case study

The latest version of INCA-P retains many of the same process representations as previous versions of the model, meaning that existing studies still provide useful demonstrations of a number of model processes; these are not therefore re-examined here. For example, previous studies have focused on soil erosion and sediment transport (Lazar et al., 2010), in-stream macrophyte and epiphyte processes (Wade et al., 2001) and shorter term TDP and PP dynamics (Jackson-Blake et al., 2015). In this case study application we therefore focus on two of the processes which have changed in the latest version: (1) PP dynamics, comparing output from the latest version of the model to output from v1.0.2, and (2) the longer-term soil P and soil water TDP simulation, as the new dynamic EPC_0 calculation (e.g. Equation 6) makes it possible to simulate long-term

soil and stream bed sediment P content and associated TDP concentrations. The focus here is on the soil compartment, rather than in-stream processing, as net fluxes associated with the latter are thought to be minor in this catchment (Jackson-Blake et al., 2015).

3.2 Methods

3.2.1 Study area and spatial set-up

The Tarland catchment (51 km^2) is a rural sub-catchment of the River Dee in northeast Scotland (WGS84 57.11, -2.80). For the period 2000-2010, mean annual rainfall was 966 mm and mean stream discharge was 0.73 m^3 s^{-1} (451 mm yr^{-1}). The stream was split into four reaches and associated sub-catchments (Figure 3), based on the location of monitoring points and effluent discharges. Landscape units were based solely on land cover, as there is a reasonable correspondence between soil and land cover in the catchment: humus iron podzols and cambisols (brown forest soils) predominate under all but semi-natural land, where peaty podzols also become important on the hill tops fringing the catchment. Three land cover classes were used, merging classes from the Land Cover Map of Scotland (LCM2007): (1) semi-natural, including upland heath, forestry and rough grazing; (2) improved grassland (temporary and permanent) and (3) arable (primarily spring barley, but also other crops and set-aside). Reach and sub-catchment properties are given in Table 4.

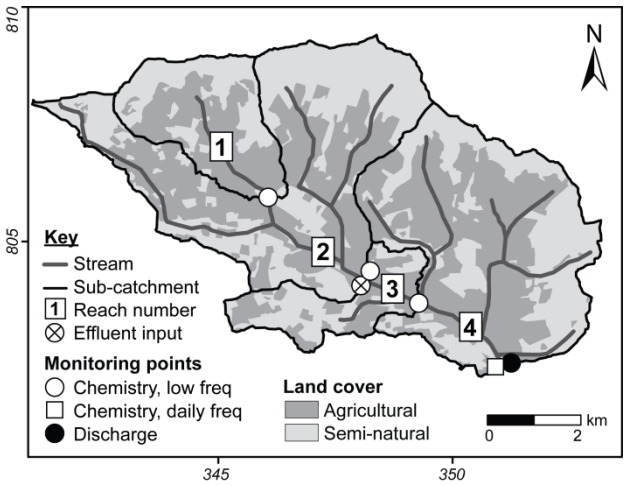

Figure 3: The Tarland catchment with reaches and associated sub-catchments used in the INCA-P set-up. Monitoring data points and land use are also shown. Eastings and northings (km) are relative to the British National Grid.

Reach	Reach length (km)	Sub-catchment area (km^2)	Land use (%)			Soils (%)			
			Arable	Improved grassland	Semi-natural	Brown forest soil	Humus iron podzol	Peaty podzol	Alluvial & gleys
1	2.8	7.2	24.2	32.8	43.0	60	20	16	4
2	2.9	19.6	19.6	29.4	51.0	52	27	13	8
3	1.3	4.4	13.3	40.5	46.2	2	77	0	21
4	2.3	19.4	23.1	34.1	42.8	33	40	10	17

Table 4: Reach and sub-catchment properties.

3.2.2 Data for model parameterisation, calibration and testing

Discharge and water chemistry data are available from the catchment outflow for the period 2000 – 2010. Sparser water chemistry data are also available from three other points along the main stem (Figure 3). At the catchment outflow, weekly sampling took place between 2000 and the end of 2003, with some daily sampling

during rainfall events. Daily samples were then collected between February 2004 and June 2005, providing 15 months of daily data. After June 2005, infrequent irregular sampling took place for the rest of the period. Measured determinands include suspended sediment (SS), total dissolved P (TDP) and soluble reactive P (SRP) concentration; the daily 2004-2005 samples were also analysed for total P (TP), allowing particulate P (PP) to be calculated (as TP – TDP). For further details of monitoring and analytical methods, see Stutter et al. (2008).

Input time series of air temperature and precipitation were derived from the Met Office 5 km gridded dataset; HER and SMD were generated using a simple water balance model (Jackson-Blake et al., 2015). A comprehensive set of additional data were compiled to help parameterise the model, including fertilizer and manure application rates (Table 5), estimates of maximum annual plant uptake of P (Table 5), sewage effluent inputs (Table 5), one-off measurements of soil solution TDP concentration from soil core leachate (Stutter et al., 2009a), observed regional groundwater TDP concentrations (Smedley et al., 2009) and soils data, including soil TP content and bulk density from the Scottish Soils Knowledge and Information Base (SSKIB; Lilly et al., 2004). See Jackson-Blake et al. (2015) for a full description of these data sets.

a) Terrestrial annual P inputs and outputs via plant uptake (kg ha^{-1} yr^{-1}):

Land use class	*Fertilizer & manure inputs*	*Maximum net plant uptake*	*Annual excess*
Arable	23	13	10
Improved grassland	26	15	11
Semi-natural	0	0	0

b) Sewage effluent inputs to the study reaches:

Reach	*P concentration (mg l^{-1})*	*Discharge (m^3 s^{-1})*
1	6.2	2.8×10^{-5}
2	6.2	7.5×10^{-5}
3	3.0	1.3×10^{-3}
4	6.2	7.5×10^{-5}

Table 5: a) Assumed annual P inputs to the land phase from fertilizer and manure and annual net plant uptake. The resulting annual balance is also provided. b) Sewage inputs, combining inputs from septic tanks and a sewage treatment works.

3.2.3 Simplified model set-up and associated assumptions

Within a given catchment, many of the processes in INCA-P are likely to be either relatively unimportant, or there may be insufficient data for the processes to be included in a meaningful way. To reduce model complexity and data requirements, simplifying assumptions can often therefore be made. Here, the following assumptions were made:

1) The labile and inactive soil P stores were assumed to be independent over the relatively short time period of interest, and therefore chemical immobilization and weathering rates were set to zero.
2) In semi-natural Scottish uplands, plant communities are P limited or N and P co-limited (Britton and Fisher, 2007) and soil and associated surface waters have very low dissolved P concentrations throughout the year (Q75<5 μg l^{-1}; unpublished James Hutton Institute data). This implies tight biological cycling, so in the semi-natural land class net uptake, plant residue inputs, deposition inputs and leaching outputs were assumed to be in balance and were set to zero. Soil water TDP

concentrations were assumed to be around zero and all soil P in semi-natural land was assumed to be in the inactive store.

3) In agricultural land, the inactive soil P store was assumed to be the same as in semi-natural land, and the difference between cultivated and semi-natural total P content (SSKIB data) was assumed to be labile P. This assumption means that simulated soil water TDP concentration in agricultural soils will decrease to semi-natural values (i.e. near zero) as total soil P approaches the value in semi-natural land and soil labile P drops to zero. This assumption is only valid if soils under the two land classes are of the same type and in the same pedological development stage. This is likely here, as the difference between semi-natural and agricultural soil P was calculated for two soil series which are widespread under both cultivated and semi-natural land in the catchment (Countesswells and Tarves). SSKIB reports soil P content for both cultivated and semi-natural soil profiles for both series, and it was assumed that within-series differences are due to human factors. The final inactive soil P value used (873 mg kg^{-1}) is an average of this difference for the two series, giving an initial labile soil P content on agricultural land of 585 mg kg^{-1}.
4) Literature-derived estimates of P inputs and plant uptake values were very similar for improved grassland and arable land use classes, and there was no data to distinguish between the soil total P content in the two classes. They were therefore identically parameterised using average values, apart from the soil erodibility parameter (to allow for a difference in the SS and PP flux from the two classes).
5) Daily or seasonal variations in soil water TDP concentration in response to fertilizer and manure inputs and plant uptake did not result in improved model performance compared to a model set-up with a relatively constant soil water TDP concentration (over sub-annual time scales). This is not surprising, as P applied in fertilizer and manure is rapidly incorporated into the soil structure and then re-released throughout the year as plant uptake and leaching remove P from the soil solution (e.g. Sisák, 2009). For simplicity, it was therefore assumed that fertilizer and manure applications and plant uptake occurred at a constant rate throughout the year, with inputs in liquid form. This satisfies the annual P balance and results in a relatively constant soil water TDP concentration (at a sub-annual time scale). An alternative approach would be to set the sorption scaling factor, K_{soil}, to a large value to simulate the rapid sorption of much larger pulses of fertilizer and manure P (in this set-up it was assumed to equal one).
6) Sorption reactions control TDP concentrations in soil waters, so the sorption equations (Equation 5 and Equation 6) must be carefully parameterised. A simple linear relationship between adsorbed P mass in the soil (mg kg^{-1}) and the soil water EPC_0 ($EPC_{0,soil}$) was assumed, as recommended by McCray et al. (2005). Practically, this involves setting the Freundlich isotherm constant, $n_{f,soil}$, to 1. The gradient of the line ($K_{f,soil}$, the sorption coefficient) can then be estimated if two points on the line are known. These two points were obtained by assuming that when soil labile P content = 585 mg kg^{-1} (agricultural land), $EPC_{0,soil}$ = 0.1 mg l^{-1} (calibrated from within the likely range in the catchment), and that the line passes through the origin (semi-natural land). This gives a $K_{f,soil}$ of 5850 l kg $soil^{-1}$ for the calibrated soil depth (Section 3.2.4).
7) Groundwater was assumed to have a constant TDP concentration of 0.01 mg l^{-1}, fitting with regional observations (Smedley et al., 2009).
8) Sediment generation on land was simplified to just occur via flow erosion; splash detachment was not considered. The soil grain size distribution was also simplified to just one size class, silt (2 – 60 μm), which most closely corresponds to the effective particle size distribution of suspended sediment measured across a suite of rivers (Marttila and Kløve, 2015; Walling and Woodward, 2000).

9) In this catchment, in-stream TDP concentrations are primarily controlled by delivery from the land phase and effluent inputs, rather than by in-stream processing (Jackson-Blake et al., 2015). The only in-stream processes included were therefore entrainment and deposition of sediment and associated PP.
10) The majority of parameters were assumed to be the same across land use types, sub-catchments or reaches, the main exceptions being GIS or measurement-derived parameters and terrestrial parameters responsible for controlling the differences in simulated nutrient or sediment fluxes between the different land use classes.

3.2.4 Model calibration and validation

The model was calibrated for the period 2004-2005, using 15 months of daily discharge and surface chemistry data from reach 4. The model was then tested against daily discharge data and sparser water chemistry data for the 11 year period 2000-2010, excluding 2004-2005.

The model was calibrated manually rather than using an auto-calibration algorithm. Auto-calibration is time-consuming, and in the case of complex models like INCA-P it is questionable whether better or more robust results are obtained than when manual calibration is used (discussed more fully in Jackson-Blake and Starrfelt, 2015). Calibration was first carried out for the two year calibration period. This was done in a step-wise manner: hydrology-related parameters were adjusted until an acceptable discharge calibration was obtained, then sediment-related parameters and finally P-related parameters, with smaller iterations of altering the hydrology and sediment parameters to improve the P simulation. Additional data taken into account in model calibration included likely soil solution TDP concentrations in the catchment. There are no widely-accepted criteria for determining whether P model performance is acceptable, and so a combination of model evaluation measures were used (Jackson-Blake et al., 2015), including: (1) visual assessment of time series, (2) comparison of distributions of observed and simulated data using Q-Q plots, and (3) model performance statistics, including Spearman's Rank correlation coefficient and model bias (%). Nash Sutcliffe efficiency (NS) and R^2 (Pearson's product moment correlation coefficient squared) were also used for discharge, with a requirement for $NS > 0.65$ for model performance to be classed as acceptable (Moriasi et al., 2007). In addition, the calibration procedure included checking for plausible changes in groundwater volume, soil P mass and stream bed sediment and PP mass during the course of the model run.

The calibration procedure then involved adjusting several parameters which do not affect the shorter term simulation, but do affect the longer term behaviour of soil P. Elevated stores of soil P can undermine attempts to reduce in-stream P concentrations potentially for decades after reductions in P inputs to land (Sharpley et al., 2013). To simulate this legacy P effect, soil P status must change in response to changing P inputs at a sensible rate. This rate was determined from long-term monitoring experiments, which have shown that when P fertilization of agricultural land ceases, soil P content appears to decay exponentially with a half-life of 7 to 9 years (e.g. McCollum, 1991; Syers et al., 2008). Within the model, the simulated rate of change in soil labile P depends on the initial soil labile P store, sorption reaction rates and plant uptake rates. The initial labile P mass is controlled by soil depth, bulk density and initial labile P concentration. Soil depth was considered to be the most uncertain of these, and so to ensure a sensible result from scenario analyses, soil depth was calibrated to ensure that, in the absence of P inputs and with plant uptake rates set at values typical for semi-natural land, soil labile P in agricultural land dropped to near zero within 35 years (assuming the more conservative half-life of 9 years). The result was an effective soil depth of 7 cm; 14 cm taking soil porosity

into account. This is plausible, given that soil P content decreases with depth and is highest in the top 20 cm in agricultural soils (Syers et al., 2008).

3.2.5 Scenario analysis

The calibrated model was run for a 30-year period to provide a baseline dataset: initial conditions were set equal to the calibration run (i.e. for 2004), then the model was run using input data for the period 1981-2010. Simple fertilizer/manure reduction measures were then simulated, including 25%, 50% and 100% reductions in P inputs. A 25% reduction in P inputs is a potentially realistic management option for the catchment, whilst the 50% and 100% reduction options are unlikely to be implemented in reality, and serve as sensitivity tests for the model. Soil P content and soil water and in-stream TDP concentrations were then compared for the baseline and scenario runs.

3.3 Case study results and discussion

3.3.1 Model calibration and validation results

Catchment P models tend to perform well in areas where point sources provide the dominant P input, but struggle in rural areas where inputs are more diffuse (Jackson-Blake et al., 2015; Wade et al., 2007). Given the rural setting of the Tarland, model performance statistics for TDP and PP (Table 6) were therefore reasonable, with significant positive correlations between observed and simulated data and percent bias <45% for all variables in both the calibration and validation periods (Moriasi et al., 2007). NS statistics are reported due to their prevalence in the literature, but are poor at discriminating between plausible and implausible TDP and PP simulations in rural areas (discussed further in Jackson-Blake et al., 2015), and are therefore not considered further here.

As mentioned in Section 3.1, model performance in the study catchment with respect to TDP was examined in Jackson-Blake et al. (2015), so only a brief description is given here. Simulated TDP concentrations were generally of the right magnitude during baseflow, increasing by the right order around rainfall events (Figure 4 and Figure 5). Simulated concentrations were not as responsive to small rainfall events as observed data, resulting in fewer peaks, and the peaks that were simulated tend to be broader than observed. This is thought to be because of issues with the driving HER time series, the lack of TDP in quick flow generated via infiltration excess, and more generally because of the limitations of using a semi-distributed model. Meanwhile, the model over-estimated the lowest TDP concentrations (Figure 6). This may be partly due to the lack of a snow module in the hydrology model used to generate the input HER time series.

For PP, the issue of under-simulated peaks was more pronounced, likely due to the more diffuse and sporadic nature of PP (and associated SS) inputs. However, the simulated PP dynamics were closely linked to simulated SS dynamics and in-stream discharge, in contrast to the model application in this catchment using v1.0.2 (Jackson-Blake et al., 2015). Simulated increases in discharge and SS concentration were accompanied by increases in PP concentration, as expected (Figure 4); in the previous application this was not the case (dashed line on Figure 4). This more realistic PP behaviour is reflected in the improved correlation coefficient (Table 6); in the previous application there was no significant correlation between observed and simulated data (bracketed values in Table 6). This new model version therefore represents a substantial improvement over previous versions. Simulated summer PP concentrations are still however problematic, with under-estimation of PP between ~3 and 20 $\mu g\ l^{-1}$ (Figure 6). This may be because organic matter generated in-stream, such as sloughed biofilms, may make up an important amount of PP during summer (Stutter et al.,

2009b), and is not accounted for in the model. This may be something to consider adding in the future, although more summer PP data would be needed to confirm that this is an issue.

Whilst the model produces plausible TDP and PP simulations in the study catchment, there is a need for further testing in a variety of areas and with applications at different scales. A particularly useful test would be to compare model output to edge-of-field PP and TDP monitoring data, to determine whether the simulated soil P processes are reasonable in agricultural areas.

Var	Calibration					Validation				
	N	Bias (%)	Spearman's Rank	NS	NS (logs)	N	Bias (%)	Spearman's Rank	NS	NS (logs)
Q	716	0.0	0.91*	0.73	0.79	3213	12	0.87*	0.55	0.72
SS	448	-16	0.46*	0.02	0.34	189	-43	0.31*	0.05	0.33
TP	428	-14	0.37*	0.07	0.13					
PP	428	-43	0.28*	0.01	-0.06					
		(-27)	(0.07)	(-0.04)						
TDP	449	9.1	0.34*	-0.24	-0.14	105	6.5	0.44*	0.10	0.17

*: significant, $p<0.001$. Otherwise not significant ($p\geq0.05$). N: number of observations; NS: Nash Sutcliffe efficiency

Table 6: performance statistics for INCA-P v1.4.4 for the calibration and validation periods, reach 4. Bracketed values for PP relate to results from INCA-P v1.0.2.

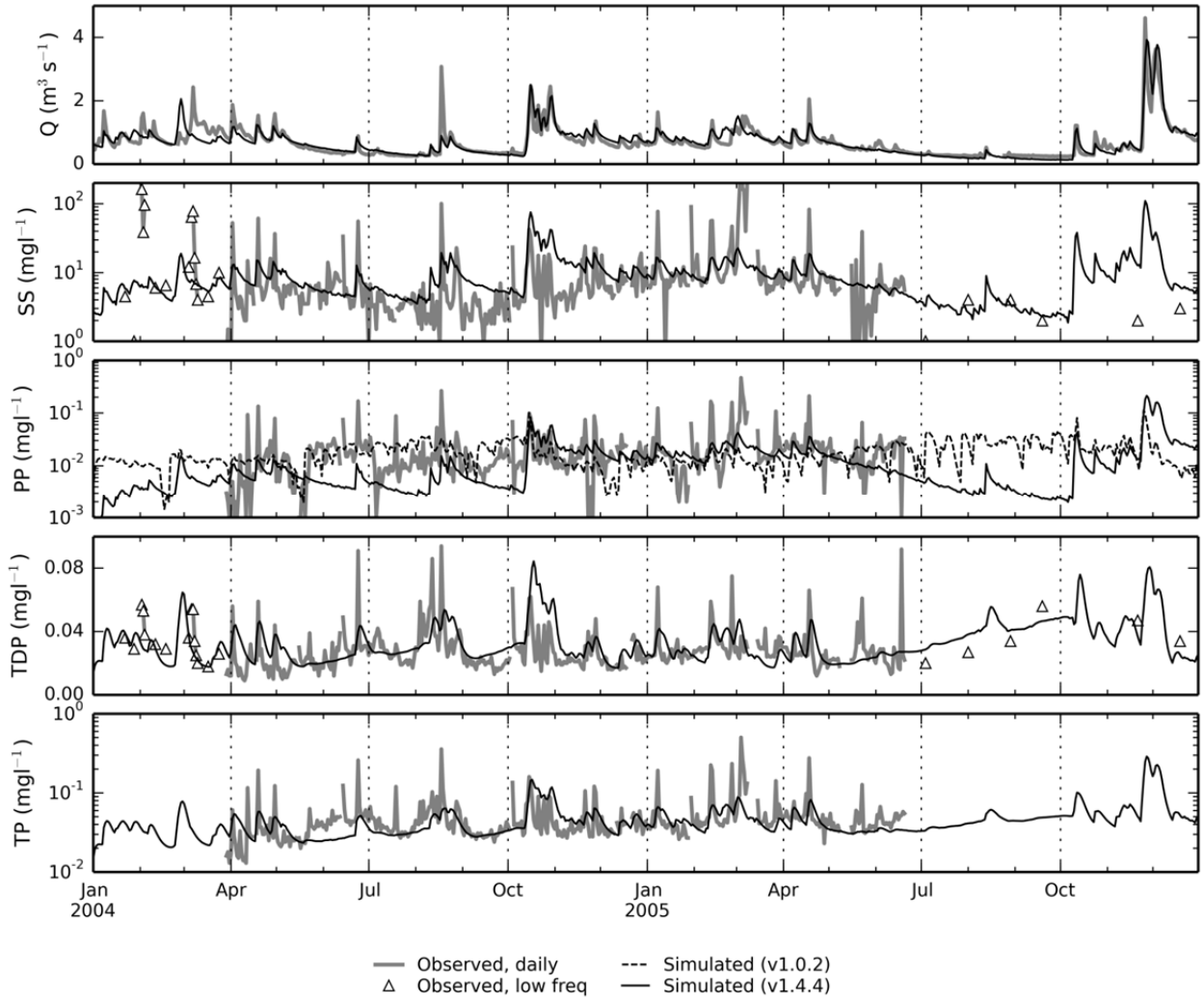

Figure 4: Time series of simulated and observed data for the calibration period, reach 4. Note the log scale for all but Q and TDP. For PP, model output from two INCA-P versions is shown (solid and dashed lines).

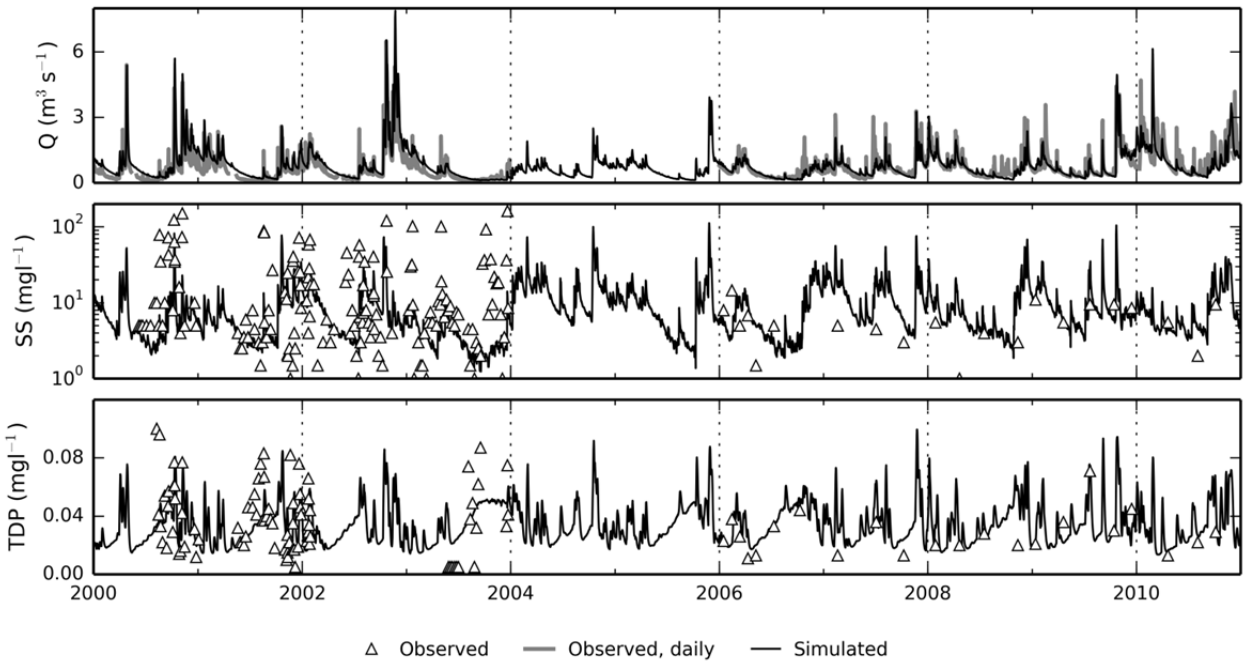

Figure 5: Time series of simulated and observed data for the validation period, reach 4. Note the log scale for SS.

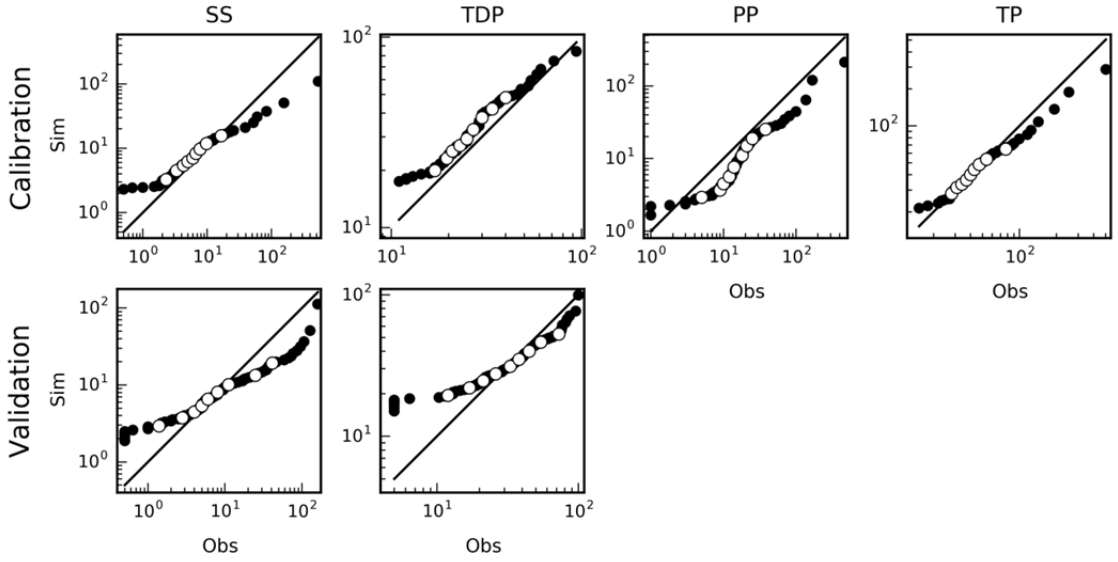

Figure 6: Q-Q plots for reach 4 for the calibration and validation periods. Quantiles of the simulated data are plotted against the corresponding quantiles of the observed data; if observed and simulated data are from similar distributions, points will lie close to the diagonal line 1:1 line. Deciles are marked with open symbols. Units are mg l^{-1} for suspended sediment (SS) and µg l^{-1} for all P species. Note log scales.

3.3.2 Scenario analysis results

Under the baseline scenario, the continuing P surplus on agricultural land resulted in an increase in soil P content during the 30-year period, with a corresponding increase in EPC_0 (Table 7). This lead to an increase in simulated soil water TDP concentration (Figure 7) and therefore an increase in peak TDP concentrations in the stream (Figure 7), resulting in an increase in annual mean TDP concentration of 6.4 µg l^{-1} over the 30 year period (Table 8). Of the three fertilizer and manure reduction options, the smallest 25% reduction still resulted in a net annual P surplus on agricultural land, with an accompanying increase over the 30-year period in soil labile P content and soil EPC_0 (Table 7), soil water TDP concentration and in-stream TDP concentration (Figure 7). Only by the 50% P reduction option did simulated soil P content decrease over the study period, with a corresponding decrease in soil water and in-stream TDP concentration.

The model provides an indication of the time required for improvements to be noticeable. During the first five years, mean annual in-stream TDP concentrations were reduced by less than 15% compared to the baseline, even for the 100% P input reduction option (Table 8). However, by the end of the simulation period the soil-water system had re-equilibrated to the new P input values, resulting in much greater reductions in in-stream TDP concentrations. For example, the 100% reduction option resulted in a 50% reduction in mean annual in-stream TDP concentration (Table 8), with agricultural soil water TDP concentrations close to semi-natural values and stream P inputs primarily from sewage effluent and groundwater. This kind of information could be useful for helping manage expectations for when returns on investments might be achieved, or for deciding which measures to implement (e.g. measures with a faster response time might be preferred).

The simulated reductions in terrestrial P inputs bring about reductions in soil water TDP concentrations, and therefore only reduced in-stream TDP concentrations during flow peaks; baseflow concentrations were largely unaffected (Figure 7). In-stream ecology is more affected by summer baseflow P concentrations than by short-lived peaks and concentrations outside the growing season (Stamm et al., 2013), so these results suggest little

improvement in in-stream ecological status would be expected, even under the most extreme fertilizer reduction scenario. However, the associated reduction in loading from the Tarland Burn to the more ecologically-sensitive River Dee could be beneficial.

Several issues need to be kept in mind when interpreting these results. Firstly, plant P uptake is not linked to soil P content, so results assume that P uptake remains unchanged despite decreasing inputs. This is likely to be the case until soil P becomes limiting, when we might expect plant yield and P uptake to start to decrease; further work is required to determine whether this effect should be included in the model, and if so how to link critical soil test P values with total or labile soil P content simulated by the model. Secondly, the simulated soil P response times are controlled by the choice of model parameters, which were in turn chosen to provide a realistic response time based on available monitoring data (Section 3.2.5). The robustness of the results therefore depends on the quality of the data used to help inform model parameterisation, and the transferability of this data to the study catchment. Finally, reductions in fertilizer and manure application rates may have a greater impact than simulated, through a reduction in wash-off of freshly-applied fertilizer and manure, which is not simulated in the model at present (see Section 4).

Variable	Reduction in terrestrial P inputs (%)	Value, year 1	Value, year 30	Total change	Annual change
EPC_0 ($\mu g\ l^{-1}$)	0	100	157	57	1.9
	25	100	122	22	0.7
	50	100	89	-11	-0.4
	100	100	21	-79	-2.6
Soil labile P ($mg\ kg^{-1}$)	0	585	917	332	11.1
	25	585	712	127	4.2
	50	585	519	-66	-2.2
	100	585	125	-460	-15.3

Table 7: Results from the 30 year simulations in terms of EPC_0 and soil labile P content in agricultural soils

Reduction in fertilizer & manure P inputs (%)	Years 1 – 5		Years 25 – 30	
	5 yr mean ($\mu g\ l^{-1}$)	Difference to baseline (%)	5 yr mean ($\mu g\ l^{-1}$)	Difference to baseline (%)
0 (baseline)	33.4	NA	39.8	NA
25	32.4	-3	34.6	-13
50	31.5	-6	29.8	-25
100	29.6	-12	20.1	-50

Table 8: Effectiveness of mitigation measures in terms of mean annual concentrations of TDP at the catchment outlet

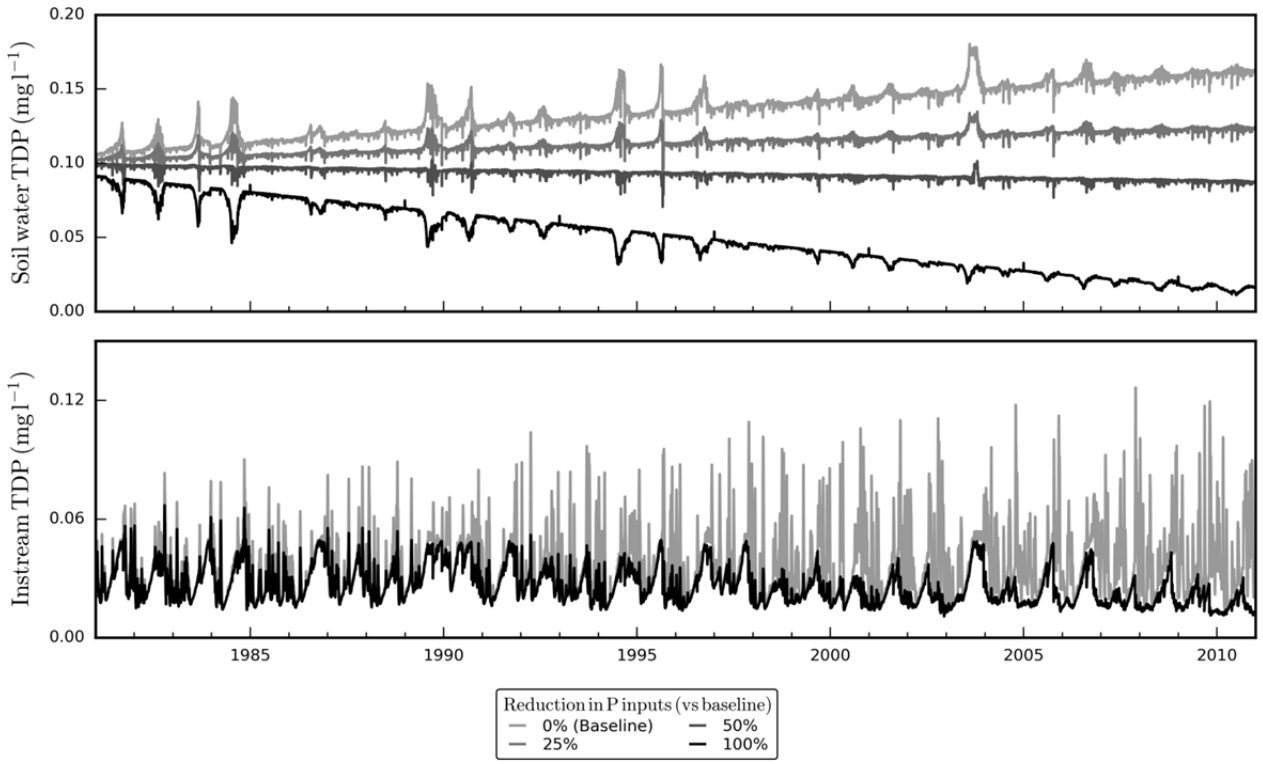

Figure 7: Time series of simulated total dissolved phosphorus (TDP) concentration in the soil water (top panel) and in-stream (bottom panel) for the 30 year simulation period. Only the baseline and 100% scenarios are shown in the bottom panel, to provide an envelope for the likely response.

4. Model applicability and limitations

The model aims to include the key processes that could affect catchment-scale P mobilisation, transport and retention within a given area. This approach results in a flexible model which can be applied at a broad range of spatial and temporal scales, making it particularly suitable for use as a research tool. It could be used, for example, to formulate hypotheses about the dominant processes and pathways within a catchment, to highlight data gaps that could help differentiate between hypotheses, or to examine how water quality might vary spatially and temporally, for example in response to climate, land use, demographic change or longer-term changes in the terrestrial P balance. One of the main advantages of the model is that it can be used to simulate both short-term, event-based dynamics, and longer-term dynamics (as demonstrated in the case study).

The downside of the flexible model structure is a relatively complex model, although it is comparable in complexity to similar models (e.g. SWAT and AnnAGNPS) and is simpler than fully distributed approaches such as MIKE-SHE (Refsgaard et al., 1995). Within a given system it is very likely that the model will be insensitive to many of the simulated processes. A certain amount of model simplification is therefore likely to be possible and indeed desirable (e.g. Section 3.2.3), but must be carried out with full awareness of model processes and assumptions. In this application, even a simplified set-up still required a large number of parameter values to be supplied, and a high level of familiarity with the model. As discussed in Jackson-Blake and Starrfelt (2015), the large number of model parameters means that a thorough exploration of the parameter space is infeasible, and therefore further simplification is required before full sensitivity and uncertainty analyses and automated calibration can be carried out in a reasonable time frame.

Despite its relative complexity compared to data availability in many areas, the model still takes a simple approach to P chemistry, ignoring the influence that the wider biogeochemical environment can have on P

mobilisation, cycling and transport. For example, the role that carbon and other nutrients play in mediating biological P uptake and in controlling mineralization and immobilisation rates (Reddy et al., 1999) is not included, inorganic and organic P processes are lumped together, soil biotic and abiotic processes are grouped, a constant SRP:TDP ratio is assumed, and the important effect redox, pH and soil and sediment texture and mineralogy may exert on P mobility are omitted. These simplifications mean that it becomes difficult to assign physical meaning to model parameters such as Freundlich sorption parameters, or to simulated variables such as soil labile P content. Further model testing, for example using edge-of-field monitoring data spanning changing soil P conditions, is required to determine whether these simplifications are justified, and further model development may be required to improve the compatibility of model parameters and output with more widely-available or agronomically-relevant data (e.g. soil test P data and SRP concentrations).

Other more specific issues which might limit model applicability in certain circumstances include:

- The semi-distributed spatial conceptualisation of a catchment requires the assumption that initial conditions, P inputs, transformations and output fluxes are the same within a given landscape class, irrespective of location within the catchment. This reduces model complexity and run times and is often proportionate to the amount of data available, but results in the spatial averaging of often highly disparate biogeochemical processes, flow pathways and farming practices. In addition, the hydrological connectivity of the landscape is not modelled as it is in fully distributed approaches. This means that the model is not particularly well suited to looking at critical source areas, for example, or the effectiveness of edge-of-field measures aimed at reducing diffuse pollution.
- Rainfall events may wash freshly applied fertilizers or manures from the soil surface to water courses. Such 'incidental' P losses from the land surface may be very important in some areas (e.g. Withers et al., 2003), but a lack of data means they are difficult to include in a catchment-scale model in a meaningful way. They are not therefore explicitly accounted for in INCA-P at present, as it is assumed that all P inputs to the land are incorporated into the soil. This means that the model cannot easily simulate the effectiveness of measures aimed at reducing incidental losses. Several models have been developed in recent years to simulate incidental P losses (e.g. Vadas et al., 2011; Vadas et al., 2008), which could form the basis of future improvements to INCA-P.
- Catchment water quality models such as INCA are frequently required to simulate the effect of water protection measures. Aside from issues with simulating measures to reduce edge-of-field and incidental losses (mentioned above), this is possible provided that data or knowledge is available on how much a certain measure will affect a process or flux already included in INCA-P. The model is therefore best suited to examining the impact of broad-scale measures such as land use change and changing terrestrial P inputs. Other processes may be simulated, but are likely to be much more uncertain due to both a lack of knowledge of the true effectiveness of a measure in a given location, combined with the spatial averaging brought about by using a semi-distributed set-up. The difficulties in simulating more detailed land management measures limits the model's utility for informing land management directly, as decisions are often made at scales which are too fine for the model (i.e. field and farm scale). However, catchment models like INCA are useful for integrating the effectiveness of measures over larger catchment scales of ecological interest, e.g. to predict whether reductions in inputs in one sub-catchment are likely to bring about desired changes down-stream given the other hydrological and P inputs, as well as the potential time to see improvements. The model may also inform management measures by profiling the dominant processes or pathways in the catchment,

which in turn provides information on the kinds of measures to prioritise in an area; more spatially-explicit GIS or field/farm-scale modelling could then be used to develop management plans.

- To date, the model has been applied in a range of catchments across northern Europe, Canada and in northern India, and is expected to be applicable across a range of environmental conditions. However, the model equations assume fairly temperate conditions and uncomplicated hydrology. Poor performance would therefore be expected in areas where this is not the case, such as karstic terrain or ephemeral water courses.
- Because the impact of redox and pH on P mobility are not taken into account in the model, it is unlikely to perform well in catchments fed by anaerobic, Fe-rich groundwater. For example, in many delta systems, the strong redox and pH gradient at the groundwater-surface water interface leads to rapid oxidisation of Fe^{2+}, resulting in the precipitation of iron oxyhydroxides with co-precipitation of phosphate, and a corresponding reduction in P availability in surface waters (Baken et al., 2015; Van der Grift et al., 2014).
- The in-stream biological equations were developed for application in chalk streams in southern England, where macrophytes abound and are the primary substrate for epiphytic algae. The in-stream biological equations cannot account for P uptake by benthic algal mats, which may be significant (Reddy et al., 1999), and there is no subsequent mineralization of P sequestered in biomass. The in-stream biological response is only controlled by temperature and P concentration, ignoring the effect of discharge and concentrations of other nutrients. This is a future model development need, and could for example help in improving the summer PP simulation in areas where sloughed biofilms make up a significant proportion of the in-stream PP (Section 3.3.1).

For the model to produce realistic results, good quality data must be available for model calibration and validation. Indeed, as with all mechanistic models, INCA-P should only be used to advise policy and land management if internal processes and parameters are sufficiently well-constrained that the modeller can be confident that the right processes are being captured. This requires data to constrain parameter values and internal fluxes within the catchment, as well as standard 'end-of-pipe' water quality data. Without good data and process understanding, there is a real risk of obtaining results which appear reasonable but have little predictive value. Finally, long-term monitoring datasets provide the only means of parameterising and testing longer term predictions from dynamic models. Such monitoring data is relatively uncommon, and more effort is required in this area. More testing of longer term model predictions is crucial in building confidence that model output is reliable, which in turn is required for model results to be used to advise policy and land management.

Acknowledgements

Many people have contributed to model development over the years. These include I. Bärlund, P. Durand, K. Granlund, M. Hutchins, I. Huttunen, N. Jarritt, T. Karvonen, Ø. Kaste, A. Lazar, M. Paasonen-Kivekäs, T. Peltovuori, O.-P. Pietiläinen, T. Saloranta, A. Taskinen, S. Tattari, A. Vasiljev and M. Yli-Halla. Thanks to R. Helliwell and R. Skeffington for providing constructive comments on the text. Thanks also to various funding bodies, including the Nordforsk e-sciences tools and techniques project 74306, the EU FP6 Eurolimpacs project, the EU FP7 REFRESH and MARS projects (Grant agreements GOCE-CT-2003-5055409, 244121 and 603378, respectively), Environment Canada, the Ontario Ministry of the Environment and the Scottish Government's RESAS Division.

References

Anderson, H., Futter, M., Oliver, I., Redshaw, J., and Harper, A. (2010). "Trends in Scottish river water quality," Scottish Environment Protection Agency.

Baken, S., Verbeeck, M., Verheyen, D., Diels, J., and Smolders, E. (2015). Phosphorus losses from agricultural land to natural waters are reduced by immobilization in iron-rich sediments of drainage ditches. *Water Research* **71**, 160-170.

Baulch, H. M., Futter, M. N., Jin, L., Whitehead, P. G., Woods, D. T., Dillon, P. J., Butterfield, D. A., Oni, S. K., Aspden, L. P., and O'Connor, E. M. (2013). Phosphorus dynamics across intensively monitored subcatchments in the Beaver River. *Inland Waters* **3**, 187-206.

Bras, R. (1990). Hydrology: An Introduction to Hydrologic Science Addison-Wesley. *Boston, USA*.

Britton, A., and Fisher, J. (2007). NP stoichiometry of low-alpine heathland: Usefulness for bio-monitoring and prediction of pollution impacts. *Biological Conservation* **138**, 100-108.

Cassidy, R., and Jordan, P. (2011). Limitations of instantaneous water quality sampling in surface-water catchments: Comparison with near-continuous phosphorus time-series data. *Journal of Hydrology* **405**, 182-193.

Cohen, S. D., and Hindmarsh, A. C. (1996). CVODE, a stiff/nonstiff ODE solver in C. *Computers in physics* **10**, 138-143.

Coulson, K. (1975). Solar and terrestrial radiation: Methods and measurements. *New York, Academic Press, Inc., 1975. 343 p.* **1**.

Couture, R.-M., Tominaga, K., Starrfelt, J., Moe, S. J., Kaste, Ø., and Wright, R. F. (2014). Modelling phosphorus loading and algal blooms in a Nordic agricultural catchment-lake system under changing land-use and climate. *Environmental Science: Processes & Impacts* **16**, 1588-1599.

Crossman, J., Futter, M. N., Oni, S. K., Whitehead, P. G., Jin, L., Butterfield, D., Baulch, H. M., and Dillon, P. J. (2013). Impacts of climate change on hydrology and water quality: Future proofing management strategies in the Lake Simcoe watershed, Canada. *Journal of Great Lakes Research* **39**, 19-32.

EEA (2012). "European waters - assessment of status and pressures," European Environment Agency, Copenhagen.

EEA (2015). Nutrients in freshwater. European Environment Agency, Denmark.

Elser, J. J., Bracken, M. E. S., Cleland, E. E., Gruner, D. S., Harpole, W. S., Hillebrand, H., Ngai, J. T., Seabloom, E. W., Shurin, J. B., and Smith, J. E. (2007). Global analysis of nitrogen and phosphorus limitation of primary producers in freshwater, marine and terrestrial ecosystems. *Ecology Letters* **10**, 1135-1142.

Farkas, C., Beldring, S., Bechmann, M., and Deelstra, J. (2013). Soil erosion and phosphorus losses under variable land use as simulated by the INCA-P model. *Soil Use and Management* **29**, 124-137.

Futter, M. N., Erlandsson, M. A., Butterfield, D., Whitehead, P. G., Oni, S. K., and Wade, A. J. (2014). PERSiST: a flexible rainfall-runoff modelling toolkit for use with the INCA family of models. *Hydrol. Earth Syst. Sci.* **18**, 855-873.

House, W. A., and Denison, F. H. (2000). Factors influencing the measurement of equilibrium phosphate concentrations in river sediments. *Water Research* **34**, 1187-1200.

House, W. A., and Denison, F. H. (2002). Exchange of Inorganic Phosphate between River Waters and Bed-Sediments. *Environmental Science & Technology* **36**, 4295-4301.

Jackson-Blake, L. A., Dunn, S. M., Helliwell, R. C., Skeffington, R. A., Stutter, M. I., and Wade, A. J. (2015). How well can we model stream phosphorus concentrations in agricultural catchments? *Environmental Modelling & Software* **64**, 31-46.

Jackson-Blake, L. A., and Starrfelt, J. (2015). Do higher data frequency and Bayesian auto-calibration lead to better model calibration? Insights from an application of INCA-P, a process-based river phosphorus model. *Journal of Hydrology* **527**, 641-655.

Jarritt, N. P., and Lawrence, D. S. L. (2007). Fine sediment delivery and transfer in lowland catchments: modelling suspended sediment concentrations in response to hydrological forcing. *Hydrological Processes* **21**, 2729-2744.

Jarvie, H. P., Sharpley, A. N., Scott, J. T., Haggard, B. E., Bowes, M. J., and Massey, L. B. (2012). Within-River Phosphorus Retention: Accounting for a Missing Piece in the Watershed Phosphorus Puzzle. *Environmental Science & Technology* **46**, 13284-13292.

Jarvie, H. P., Sharpley, A. N., Withers, P. J. A., Scott, J. T., Haggard, B. E., and Neal, C. (2013). Phosphorus Mitigation to Control River Eutrophication: Murky Waters, Inconvenient Truths, and "Postnormal" Science. *J. Environ. Qual.* **42**, 295-304.

Jin, L., Whitehead, P. G., Baulch, H. M., Dillon, P. J., Butterfield, D. A., Oni, S. K., Futter, M. N., Crossman, J., and O'Connor, E. M. (2013). Modelling phosphorus in Lake Simcoe and its subcatchments: scenario analysis to assess alternative management strategies. *Inland Waters* **3**, 207-220.

Jin, L., Whitehead, P. G., Sarkar, S., Sinha, R., Futter, M. N., Butterfield, D., Caesar, J., and Crossman, J. (2015). Assessing the impacts of climate change and socio-economic changes on flow and phosphorus flux in the Ganga river system. *Environmental Science: Processes & Impacts* **17**, 1098-1110.

Kirk, J. T. (1994). "Light and photosynthesis in aquatic ecosystems," Cambridge university press.

Lazar, A. N., Butterfield, D., Futter, M. N., Rankinen, K., Thouvenot-Korppoo, M., Jarritt, N., Lawrence, D. S. L., Wade, A. J., and Whitehead, P. G. (2010). An assessment of the fine sediment dynamics in an upland river system: INCA-Sed modifications and implications for fisheries. *Science of The Total Environment* **408**, 2555-2566.

Lilly, A., Towers, W., Malcolm, A., and Paterson, E. (2004). Scottish Soils Knowledge and Information Base (SSKIB). (M. L. U. R. Institute, ed.). James Hutton Institute, Aberdeen, Scotland.

Lin, C., and Banin, A. (2005). Effect of Long-Term Effluent Recharge on Phosphate Sorption by Soils in a Wastewater Reclamation Plant. *Water, Air, and Soil Pollution* **164**, 257-273.

Martin-Ortega, J., Perni, A., Jackson-Blake, L., Balana, B. B., McKee, A., Dunn, S., Helliwell, R., Psaltopoulos, D., Skuras, D., Cooksley, S., and Slee, B. (2015). A transdisciplinary approach to the economic analysis of the European Water Framework Directive. *Ecological Economics* **116**, 34-45.

Marttila, H., and Kløve, B. (2015). Spatial and temporal variation in particle size and particulate organic matter content in suspended particulate matter from peatland-dominated catchments in Finland. *Hydrological Processes* **29**, 1069-1079.

McCollum, R. E. (1991). Buildup and Decline in Soil Phosphorus: 30-Year Trends on a Typic Umprabuult. *Agronomy Journal* **83**, 77-85.

McCray, J. E., Kirkland, S. L., Siegrist, R. L., and Thyne, G. D. (2005). Model Parameters for Simulating Fate and Transport of On-Site Wastewater Nutrients. *Ground Water* **43**, 628-639.

McIntyre, N. R., and Wheater, H. S. (2004). Calibration of an in-river phosphorus model: prior evaluation of data needs and model uncertainty. *Journal of Hydrology* **290**, 100-116.

Meals, D. W., Dressing, S. A., and Davenport, T. E. (2010). Lag Time in Water Quality Response to Best Management Practices: A Review. *J. Environ. Qual.* **39**, 85-96.

Meeus, J. (1998). Astronomical algorithms 2nd edition. *Willmann-BeII Inc. Richmond, VA*.

Moriasi, D., Arnold, J., Van Liew, M., Bingner, R., Harmel, R., and Veith, T. (2007). Model evaluation guidelines for systematic quantification of accuracy in watershed simulations. *Transactions of the ASABE* **50**, 885-900.

Rankinen, K., Karvonen, T., and Butterfield, D. (2004a). A simple model for predicting soil temperature in snow-covered and seasonally frozen soil: model description and testing. *Hydrol. Earth Syst. Sci.* **8**, 706-716.

Rankinen, K., Kaste, Ø., and Butterfield, D. (2004b). Adaptation of the Integrated Nitrogen Model for Catchments (INCA) to seasonally snow-covered catchments. *Hydrology and Earth System Sciences Discussions* **8**, 695-705.

Reddy, K. R., Kadlec, R. H., Flaig, E., and Gale, P. M. (1999). Phosphorus Retention in Streams and Wetlands: A Review. *Critical Reviews in Environmental Science and Technology* **29**, 83-146.

Refsgaard, J., Storm, B., and Singh, V. (1995). MIKE SHE. *Computer models of watershed hydrology.*, 809-846.

Sælthun, N. R. (1996). The Nordic HBV model. *Norwegian Water Resources and Energy Administration Publication* **7**, 1-26.

Sharpley, A., Jarvie, H. P., Buda, A., May, L., Spears, B., and Kleinman, P. (2013). Phosphorus Legacy: Overcoming the Effects of Past Management Practices to Mitigate Future Water Quality Impairment. *J. Environ. Qual.* **42**, 1308-1326.

Sharpley, A. N. (1980). The Enrichment of Soil Phosphorus in Runoff Sediments1. *J. Environ. Qual.* **9**, 521-526.

Sisák, I. (2009). Assessment of Short-Term and Long-Term Phosphorus Dynamics in Four Soils in the Watershed of Lake Balaton. *Communications in Soil Science and Plant Analysis* **40**, 947-959.

Smedley, P. L., Ó Dochartaigh, B. É., Macdonald, A. M., and Darling, W. G. (2009). "Baseline Scotland: groundwater chemistry of Aberdeenshire."

Stamm, C., Jarvie, H. P., and Scott, T. (2013). What's more important for managing phosphorus: loads, concentrations or both? *Environmental science & technology* **48**, 23-24.

Starrfelt, J., and Kaste, O. (2014). Bayesian uncertainty assessment of a semi-distributed integrated catchment model of phosphorus transport. *Environmental Science: Processes & Impacts* **16**, 1578-1587.

Stutter, M. I., Demars, B. O. L., and Langan, S. J. (2010). River phosphorus cycling: Separating biotic and abiotic uptake during short-term changes in sewage effluent loading. *Water Research* **44**, 4425-4436.

Stutter, M. I., Langan, S. J., and Cooper, R. J. (2008). Spatial contributions of diffuse inputs and within-channel processes to the form of stream water phosphorus over storm events. *Journal of Hydrology* **350**, 203-214.

Stutter, M. I., Langan, S. J., and Lumsdon, D. G. (2009a). Vegetated Buffer Strips Can Lead to Increased Release of Phosphorus to Waters: A Biogeochemical Assessment of the Mechanisms. *Environmental Science & Technology* **43**, 1858-1863.

Stutter, M. I., Langan, S. J., Lumsdon, D. G., and Clark, L. M. (2009b). Multi-element signatures of stream sediments and sources under moderate to low flow conditions. *Applied Geochemistry* **24**, 800-809.

Syers, J. K., Johnston, A. E., and Curtin, D. (2008). Efficiency of soil and fertilizer phosphorus use. Reconciling changing concepts of soil phosphorus behaviour with agronomic information. *In* "Fertilizer and plant nutrition bulletins", pp. 123. Food and Agriculture Organisation of the United Nations (FAO), Rome.

Vadas, P. A., Aarons, S. R., Butler, D. M., and Dougherty, W. J. (2011). A new model for dung decomposition and phosphorus transformations and loss in runoff. *Soil Research* **49**, 367-375.

Vadas, P. A., Owens, L. B., and Sharpley, A. N. (2008). An empirical model for dissolved phosphorus in runoff from surface-applied fertilizers. *Agriculture, Ecosystems & Environment* **127**, 59-65.

Van der Grift, B., Rozemeijer, J., Griffioen, J., and van der Velde, Y. (2014). Iron oxidation kinetics and phosphate immobilization along the flow-path from groundwater into surface water. *Hydrology and Earth System Sciences Discussions* **11**, 6637-6674.

Wade, A. J., Butterfield, D., Griffiths, T., and Whitehead, P. G. (2007). Eutrophication control in river-systems: an application of INCA-P to the River Lugg. *Hydrol. Earth Syst. Sci.* **11**, 584-600.

Wade, A. J., Durand, P., Beaujouan, V., Wessel, W. W., Raat, K. J., Whitehead, P. G., Butterfield, D., Rankinen, K., and Lepisto, A. (1999). A nitrogen model for European catchments: INCA, new model structure and equations. *Hydrol. Earth Syst. Sci.* **6**, 559-582.

Wade, A. J., Hornberger, G. M., Whitehead, P. G., Jarvie, H. P., and Flynn, N. (2001). On modeling the mechanisms that control in-stream phosphorus, macrophyte, and epiphyte dynamics: An assessment of a new model using general sensitivity analysis. *Water Resources Research* **37**, 2777-2792.

Wade, A. J., Whitehead, P. G., and Butterfield, D. (2002a). The Integrated Catchments model of Phosphorus dynamics (INCA-P), a new approach for multiple source assessment in heterogeneous river systems: model structure and equations. *Hydrol. Earth Syst. Sci.* **6**, 583-606.

Wade, A. J., Whitehead, P. G., Hornberger, G. M., Jarvie, H. P., and Flynn, N. (2002b). On modelling the impacts of phosphorus stripping at sewage works on in-stream phosphorus and macrophyte/epiphyte dynamics: a case study for the River Kennet. *Science of The Total Environment* **282–283**, 395-415.

Walling, D., and Woodward, J. (2000). Effective particle size characteristics of fluvial suspended sediment transported by lowland British rivers. *IAHS Publication (International Association of Hydrological Sciences)*, 129-139.

Wambecq, A. (1978). Rational Runge-Kutta methods for solving systems of ordinary differential equations. *Computing* **20**, 333-342.

Wellen, C., Kamran-Disfani, A.-R., and Arhonditsis, G. B. (2015). Evaluation of the Current State of Distributed Watershed Nutrient Water Quality Modeling. *Environmental Science & Technology* **49**, 3278-3290.

Whitehead, P. G., Crossman, J., Balana, B. B., Futter, M. N., Comber, S., Jin, L., Skuras, D., Wade, A. J., Bowes, M. J., and Read, D. S. (2013). A cost-effectiveness analysis of water security and water quality: impacts of climate and land-use change on the River Thames system. *Philosophical Transactions of the Royal Society A: Mathematical, Physical and Engineering Sciences* **371**.

Whitehead, P. G., Jin, L., Baulch, H. M., Butterfield, D. A., Oni, S. K., Dillon, P. J., Futter, M., Wade, A. J., North, R., O'Connor, E. M., and Jarvie, H. P. (2011). Modelling phosphorus dynamics in multi-branch river systems: A study of the Black River, Lake Simcoe, Ontario, Canada. *Science of The Total Environment* **412–413**, 315-323.

Whitehead, P. G., Wilson, E. J., Butterfield, D., and Seed, K. (1998). A semi-distributed integrated flow and nitrogen model for multiple source assessment in catchments (INCA): Part II — application to large river basins in south Wales and eastern England. *Science of The Total Environment* **210–211**, 559-583.

Withers, P. J., Ulén, B., Stamm, C., and Bechmann, M. (2003). Incidental phosphorus losses–are they significant and can they be predicted? *Journal of Plant Nutrition and Soil Science* **166**, 459-468.

Appendix A Hydrology equations

Water is stored in the landscape in three compartments: soil water, quick flow (primarily overland flow and tile drainage) and groundwater (Figure 2). Flow out of each store is proportional to the volume in the store, with a constant of proportionality 1/T where T is the time constant. In each store, the rate of change in volume with time is proportional to inputs minus outputs.

A.1 Terrestrial hydrology

All parameters and variables used in the terrestrial hydrology equations are defined in Table A.1.

Variable	Description	Units	Source
A_{LU}	Area of landscape class in sub-catchment	%	Input parameter
A_{SC}	Sub-catchment area	km^2	Input parameter
β	Base flow index	-	Input parameter
$C_{IExcess}$	Infiltration excess proportion to quick flow	-	Input parameter
C_{ret}	Soil water retention volume constant	-	Input parameter
C_R	Rainfall correction factor	-	Constant (1.08)
I	Infiltration rate	$m^3\ s^{-1}\ km^{-2}$	Equation A-10
I_{max}	Maximum infiltration rate	$mm\ day^{-1}$	Input parameter
q_{gw}	Groundwater flow	$m^3\ s^{-1}\ km^{-2}$	Equation A-13
$q_{gw,land}$	Groundwater flow to reach	$m^3\ s^{-1}$	Equation A-16
$q_{gw,sus}$	Groundwater sustainable flow	$m^3\ s^{-1}\ km^{-2}$	Input parameter
$q_{IExcess}$	Infiltration excess quick flow	$m^3\ s^{-1}\ km^{-2}$	Equation A-9
q_{quick}	Quick flow	$m^3\ s^{-1}\ km^{-2}$	Equation A-11
$q_{quick,land}$	Quick flow to reach	$m^3\ s^{-1}$	Equation A-17
$q_{satExcess}$	Saturation excess quick flow	$m^3\ s^{-1}\ km^{-2}$	Equation A-8
q_{soil}	Soil water flow	$m^3\ s^{-1}\ km^{-2}$	Equation A-5
$q_{soil,land}$	Soil water flow to reach	$m^3\ s^{-1}$	Equation A-15
$q_{soil,max}$	Threshold soil water flow for saturation excess	$m^3\ s^{-1}\ km^{-2}$	Input parameter
$q_{soil,sus}$	Sustainable soil water flow	$m^3\ s^{-1}\ km^{-2}$	Input parameter
$q_{soil\ out}$	Soil water flow and saturation excess	$m^3\ s^{-1}\ km^{-2}$	Equation A-3
R_{actual}	Measured actual precipitation	$mm\ day^{-1}$	Input time series
R_{eff}	Hydrologically effective precipitation	$mm\ day^{-1}$	User input timeseries
$R_{eff,q}$	Hydrologically effective precipitation flux	$m^3\ s^{-1}\ km^{-2}$	Equation A-1
$R_{rain,melt,q}$	Flux of rainfall plus snowmelt	$m^3\ s^{-1}\ km^{-2}$	Equation A-2
R_{snow}	Precipitation falling as snow	$mm\ day^{-1}$	Equation C-3
r_{user}	Input precipitation flux for infiltration calculation	$m^3\ s^{-1}\ km^{-2}$	User choice between: $R_{eff,q}$, $R_{rain,melt,q}$ or a hybrid of R_{actual} and $R_{eff,q}$
S_{Melt}	Snow melt	$mm\ day^{-1}$	Equation C-4
SMD	Soil moisture deficit	mm	Input time series
SMD_{max}	Maximum soil moisture deficit	mm	Input parameter
T_{gw}	Groundwater time constant	days	Input parameter
T_{quick}	Quick flow time constant	days	Input parameter
T_{soil}	Soil water time constant	days	Input parameter
V_{gw}	Groundwater volume	$m^3\ km^{-2}$	Equation A-14
V_{quick}	Quick flow volume	$m^3\ km^{-2}$	Equation A-12
$V_{soil\ drainage}$	Soil water drainage volume	$m^3\ km^{-2}$	Equation A-4
$V_{soil\ retention}$	Soil water retention volume	$m^3\ km^{-2}$	Equation A-6
$V_{soilwater}$	Soil water volume	$m^3\ km^{-2}$	Equation A-7

Table A.1: Parameters and variables used in terrestrial hydrology equations

A.1.1 Hydrological inputs

Hydrological processes are driven by a time series of hydrologically effective precipitation (HER), R_{eff}, which must be derived, together with soil moisture deficit (SMD), from a rainfall-runoff model (e.g. PERSiST). The

user-input HER series is converted to a flux in $m^3\ s^{-1}\ km^{-2}$, $R_{eff,q}$ (Equation A-1). To calculate infiltration excess, a time series of actual precipitation and snow melt is also calculated (Equation A-2).

Equation A-1: Hydrologically effective precipitation flux, $R_{eff,q}$ ($m^3\ s^{-1}\ km^{-2}$)

$$R_{eff,q} = \frac{10^3}{86400} R_{eff}$$

Equation A-2: Flux of rainfall plus snowmelt, $R_{rain,melt,q}$ ($m^3\ s^{-1}\ km^{-2}$)

$$R_{rain,melt,q} = \frac{10^3}{86400} (C_R(R_{actual} - R_{snow}) + S_{Melt})$$

A.1.2 Soil water

Soil water is split into a 'drainage volume', soil water above field capacity, and a 'retention volume', soil water below field capacity. The drainage volume is water which may run off to the stream, whilst the retention volume contributes to the overall volume of water in the soil, and is therefore important in calculating concentrations in the soil water.

The rate of change in flow from the O/A soil horizon, including saturation excess (Equation A-3), and the change in drainage volume (Equation A-4) are dependent on the amount of incoming effective precipitation minus outflow from the soil box. For soil water flow, the user has the option of setting a minimum threshold. The flux of water from the soil box is then corrected to take any saturation excess into account (Equation A-5), for use when calculating fluxes to groundwater. The soil water retention volume is calculated using the user-supplied soil moisture deficit (SMD) time series (Equation A-6), and the total soil water volume is then the sum of the drainage and retention volumes (Equation A-7).

Equation A-3: Change in soil water flow and saturation excess, q_{soil_out}, with time ($m^3\ s^{-1}\ km^{-2}\ day^{-1}$)

$$\frac{dq_{soil\_out}}{dt} = \frac{R_{eff,q} - q_{soil\_out}}{T_{soil}}, \text{ where } q_{soil\_out} = maximum\{q_{soil,sus}, q_{soil\_out}\}$$

Equation A-4: The change in soil drainage volume, $V_{soil\_drainage}$, with time ($m^3\ km^{-2}\ day^{-1}$)

$$\frac{dV_{soil\_drainage}}{dt} = 86400\left(R_{eff,q} - q_{soil\_out}\right)$$

Equation A-5: Corrected soil water flow, q_{soil} ($m^3\ s^{-1}\ km^{-2}$), taking saturation excess into account

$$q_{soil} = minimum\{q_{soil\_out}, q_{soil,max}\}$$

Equation A-6: Soil water retention volume, $V_{soil\_retention}$ ($m^3\ km^{-2}$). SMD_{max} must be set by the user to be greater than the maximum SMD value in the input time series.

$$V_{soil\_ret} = 10^3 C_{ret}(SMD_{max} - SMD)$$

Equation A-7: Volume of water in the soil, $V_{soilwater}$ ($m^3\ km^{-2}$)

$$V_{soilwater} = V_{soil\_drainage} + V_{soil\_retention}$$

A.1.3 Quick flow

The quick flow store has two inputs: saturation excess (Equation A-8) and infiltration excess (Equation A-9). The first step in calculating infiltration excess is to calculate the infiltration rate (Equation A-10). For this, the user may choose between using various input precipitation time series: the default is the effective precipitation flux, $R_{eff,q}$, but alternatives include actual precipitation falling as rain plus snowmelt, $R_{rain,melt,q}$, or a hybrid of actual rainfall, R_{actual}, and effective precipitation (see Lazar et al., 2010 for details). The rate of change in quick flow and volume with time are then calculated as inputs minus outputs (Equation A-11, Equation A-12).

Equation A-8: Saturation excess flow, $q_{satExcess}$ ($m^3\ s^{-1}\ km^{-2}$)

$$q_{satExcess} = maximum\{(q_{soil\_out} - q_{soil,max}), 0\}$$

Equation A-9: Infiltration excess, $q_{IExcess}$ ($m^3\ s^{-1}\ km^{-2}$)

$$q_{IExcess} = C_{IExcess}(r_{user} - minimum\{I, r_{user}\})$$

Equation A-10: Infiltration rate, I ($m^3\ s^{-1}\ km^{-2}$)

$$I = I_{max}\frac{1000}{86400}\left(1 - e^{\frac{-86.4\ r_{user}}{I_{max}}}\right)$$

Equation A-11: The change in quick flow, q_{quick}, with time ($m^3\ s^{-1}\ km^{-2}\ day^{-1}$)

$$\frac{dq_{quick}}{dt} = \frac{q_{satExcess} + q_{IExcess} - q_{quick}}{T_{quick}}$$

Equation A-12: Change in quick flow volume, V_{quick} , with time ($m^3\ km^{-2}\ day^{-1}$)

$$\frac{dV_{quick}}{dt} = 86400\left(q_{satExcess} + q_{IExcess} - q_{quick}\right)$$

A.1.4 Groundwater

The rate of change in groundwater flow (Equation A-13) and groundwater volume (Equation A-14) with time are dependent on inputs from the soil water store (O/A soil horizons) via vertical percolation to the groundwater (B/C horizons and deeper) minus outputs to the stream. An additional optional parameter ensures groundwater flow doesn't drop below a user-specified threshold.

Equation A-13: Change in groundwater flow, q_{gw}, with time ($m^3\ s^{-1}\ km^{-2}\ day^{-1}$)

$$\frac{dq_{gw}}{dt} = \frac{\beta q_{soil} - q_{gw}}{T_{gw}}, where\ q_{gw} = maximum\{q_{gw,sus}, q_{gw}\}$$

Equation A-14: Change in groundwater volume, V_{gw}, with time ($m^3\ km^{-2}\ day^{-1}$)

$$\frac{dV_{gw}}{dt} = 86400\left(\beta q_{soil} - q_{gw}\right)$$

A.1.5 Terrestrial inputs to the stream

Flows from the terrestrial compartment to the stream reach are calculated by multiplying flows for a 1km^2 cell by the sub-catchment area, taking into account how flows vary between land classes.

Equation A-15: Soil water inputs to the reach, $q_{soil,land}$ (m^3 s^{-1}), where superscript *j* denotes the landscape class

$$q_{soil,land} = \sum_{j=1}^{j=n\ land\ classes} A_{SC}\left(\frac{A_{LU}^{j}}{100}\right)(1-\beta)q_{soil}^{j}$$

Equation A-16: Groundwater inputs to the reach, $q_{gw,land}$ (m^3 s^{-1}), where superscript *j* denotes the landscape class

$$q_{gw,land} = \sum_{j=1}^{n\ land\ classes} A_{SC}\left(\frac{A_{LU}^{j}}{100}\right) q_{gw}^{j}$$

Equation A-17: Quick flow inputs to the reach, $q_{quick,land}$ (m^3 s^{-1}), where superscript *j* denotes the landscape class

$$q_{quick,land} = \sum_{j=1}^{n\ land\ classes} A_{SC}\left(\frac{A_{LU}^{j}}{100}\right) q_{quick}^{j}$$

A.2 In-stream hydrology

For each reach, the flow and volume of water in the reach are tracked (Equation A-18 and Equation A-19). Within a reach, the rate of change in water volume is proportional to inputs minus outputs and the flow out of the reach is proportional to the reach volume. The constant of proportionality is $1/T_{reach}$, where T_{reach} is the reach time constant. T_{reach} is not however constant as it is in terrestrial stores, but varies according to water velocity (Equation A-20). Water velocity is in turn determined using an empirical relationship between velocity and discharge (Equation A-21). Finally, reach depth is calculated assuming a rectangular channel cross section (Equation A-22), for use in the in-stream sediment module. Parameters and variables used in the in-stream hydrology equations are defined in Table A.2.

Equation A-18: The change in reach outflow, $q_{reach,out}$, with time (m^3 s^{-1} day^{-1})

$$\frac{dq_{reach,out}}{dt} = \frac{1}{(1-b)T_{reach}}\left(q_{reach,US} + q_{quick,land} + q_{soil,land} + q_{gw,land} + q_{eff} - q_{abs} - q_{reach,out}\right)$$

Equation A-19: The change in reach volume, V_{reach}, with time (m^3 day^{-1})

$$\frac{dV_{reach}}{dt} = 86400\left(q_{reach,US} + q_{quick,land} + q_{soil,land} + q_{gw,land} + q_{eff} - q_{abs} - q_{reach,out}\right)$$

Equation A-20: Reach time constant, T_{reach} (days)

$$T_{reach} = \frac{L_{reach}}{86400\ v}$$

Equation A-21: In-stream flow velocity, v (m s^{-1})

$$v = aq_{reach,out}^{b}$$

Equation A-22: Reach depth, d_{reach} (m)

$$d_{reach} = \frac{q_{reach,out}}{v\, w_{reach}}$$

Variable	Description	Units	Source
a	Velocity-discharge a parameter	m^{-2}	Input parameter
b	Velocity-discharge b parameter	-	Input parameter
d_{reach}	Reach depth	m	Equation A-22
L_{reach}	Reach length	m	Input parameter
q_{abs}	Reach flow abstraction	$m^3\ s^{-1}$	Input parameter/time series
q_{eff}	Reach effluent flow input	$m^3\ s^{-1}$	Input parameter/time series
$q_{gw,land}$	Groundwater flow to reach	$m^3\ s^{-1}$	Equation A-16
$q_{quick,land}$	Quick flow to reach	$m^3\ s^{-1}$	Equation A-17
$q_{reach,out}$	Reach outflow	$m^3\ s^{-1}$	Equation A-18
$q_{reach,US}$	Inflow from upstream	$m^3\ s^{-1}$	Model calculates
$q_{soil,land}$	Soil water flow to reach	$m^3\ s^{-1}$	Equation A-15
T_{reach}	Reach time constant	days	Equation A-20
v	In-stream flow velocity	m s^{-1}	Equation A-21
V_{reach}	Reach volume	m^3	Equation A-19
w_{reach}	Reach width	m	Input parameter

Table A.2: Parameters and variables used in in-stream hydrology equations

Appendix B Erosion and sediment transport equations

Sediment generation, delivery to the stream and subsequent in-stream transport and deposition are simulated as in INCA-sed with only minor alterations. The sediment equations as implemented in the INCA-P code are provided below with just a brief outline of the underlying concepts; for a full description see Jarritt and Lawrence (2007) and Lazar et al. (2010).

B.1 Terrestrial erosion and sediment delivery to the stream

All parameters and variables used in the terrestrial sediment equations are defined in Table B.1.

Variable	Description	Units	Source
a_1	Flow erosion scaling factor	s m^{-2}	Input parameter
a_2	Flow erosion direct runoff threshold	m^3 s^{-1} km^{-2}	Input parameter
a_3	Flow erosion nonlinear coefficient	-	Input parameter
a_4	Transport capacity scaling factor	kg m^{-2} km^{-2}	Input parameter
a_5	Transport capacity direct runoff threshold	m^3 s^{-1} km^{-2}	Input parameter
a_6	Transport capacity nonlinear coefficient	-	Input parameter
A_{LU}	Area of landscape class in the sub-catchment	%	Input parameter
A_{SC}	Sub-catchment area	km^2	Input parameter
C_{SD}	Splash detachment scaling factor	s m^{-1}	Input parameter
E_{FE}	Flow erosion potential	kg km^{-2} s^{-1}	Input parameter
E_{SD}	Splash detachment soil erodibility	kg m^{-2} s^{-1}	Input parameter
F_z	Percentage of sediment in grain size class *z*	%	5 input parameters
K_{FE}	Flow erosion K factor	kg km^{-2} day^{-1}	Equation B-2
L_{reach}	Reach length	m	Input parameter
m_{land}	Sediment delivery to the reach per unit area	kg km^{-2} day^{-1}	Equation B-5
$M_{land,total}$	Sediment delivery to the reach	kg day^{-1}	Equation B-6
$M_{land,total,z}$	Sediment delivery to the reach per size class, z	kg day^{-1}	Equation B-7
M_{soil}	Soil mass in the O/A horizon	kg km^{-2}	Equation B-8
q_{quick}	Quick flow	m^3 s^{-1} km^{-2}	Equation A-11
$R_{eff,q}$	Precipitation flux	m^3 s^{-1} km^{-2}	Equation A-1
S_{FE}	Flow erosion	kg km^{-2} day^{-1}	Equation B-2
S_{SD}	Splash detachment	kg km^{-2} day^{-1}	Equation B-1
S_{store}	Surface sediment store	kg km^{-2}	Equation B-3
S_{TC}	Sediment transport capacity	kg km^{-2} day^{-1}	Equation B-4
V_{index}	Vegetation index	-	Input parameter

Table B.1: Variables and parameters used in terrestrial sediment equations

B.1.1 Sediment generation

In the terrestrial compartment, sediment may be generated by splash detachment (Equation B-1) and/or by flow erosion (Equation B-2). Material generated by splash detachment enters a store of sediment on the land surface, whose mass is tracked (Equation B-3). The subsequent transport of this sediment to the stream depends on the transport capacity of overland flow (Equation B-4). Flow erosion only occurs when there is sufficient transport capacity remaining after accounting for the removal of material from the surface store.

Equation B-1: Mass of sediment mobilised via splash detachment, S_{SD} (kg km^{-2} day^{-1})

$$S_{SD} = 86400\, C_{SD} R_{eff,q} E_{SD}^{\left(\frac{10}{10-V_{index}}\right)}$$

Equation B-2: Sediment mobilisation via flow erosion, S_{FE} (kg km^{-2} day^{-1})

$$S_{FE} = \frac{K_{FE}(S_{TC} - S_{SD})}{(S_{TC} + K_{FE})}$$

$$\text{where } K_{FE} = 84600\ a_1 E_{FE} \left(\frac{A_{SC}}{L_{reach}} (q_{quick} - a_2) \right)^{a_3}$$

Equation B-3: Rate of change in mass of sediment available for transport to the stream, S_{store}, with time (kg km^{-2} day^{-1})

If $(S_{store} > 0)$ or $(S_{store} = 0 \text{ and } S_{SD} > S_{TC})$: $\frac{dS_{store}}{dt} = S_{SD} - m_{land}$

Otherwise: $\frac{dS_{store}}{dt} = 0$

Equation B-4: Sediment transport capacity, S_{TC} (kg km^{-2} day^{-1})

$$S_{TC} = 86400\ a_4 \left(\frac{A_{SC}}{L_{reach}} (q_{quick} - a_5) \right)^{a_6}$$

B.1.2 Sediment transport to the reach

The mass of sediment transported to the reach depends on the interplay between sediment generation and transport capacity, meaning that sediment transfer to the reach may be transport or source limited (Equation B-5). The overall mass of sediment transported to the reach is then calculated by summing inputs over different landscape classes and sub-catchments (Equation B-6), and finally by apportioning this total mass into the five grain sizes classes considered by the in-stream sediment model (Equation B-7). The soil mass is used in the terrestrial P sorption equations, and changes throughout the model run due to outputs via erosion (Equation B-8).

Equation B-5: Mass of bulk sediment transported to the reach per unit area, m_{land} (kg km^{-2} day^{-1})

If $(S_{store} > 0)$ or $(S_{store} = 0 \text{ and } S_{SD} > S_{TC})$: $m_{land} = S_{TC}$
Otherwise: $m_{land} = S_{SD} + S_{FE}$

Equation B-6: Mass of bulk sediment transported to each reach, $M_{land,total}$ (kg day^{-1}; superscript *j* denotes the landscape class)

$$M_{land,total} = \sum_{j=1}^{j=n\ LU\ classes} A_{SC} \left(\frac{A_{LU}^{j}}{100} \right) m_{land}^{j}$$

Equation B-7: Mass of sediment transported to the reach within each grain size class, *z*, $M_{land,total,z}$ (kg day^{-1})

$$M_{land,total,z} = \frac{F_z}{100}\ M_{land,total}$$

Equation B-8: Change in the soil mass, M_{soil}, with time (kg km^{-2} day^{-1})

$$\frac{dM_{soil}}{dt} = -m_{land}$$

B.2 In-stream

Within the in-stream sediment module, five grain size classes are considered: coarse, medium and fine sand, silt and clay. All the mass balance equations described below are calculated for each of these five grain sizes. The two key processes affecting sediment within the stream are particle deposition and resuspension, and the masses of sediment suspended in the water column and in the stream bed are tracked. All parameters and variables in the in-stream sediment equations are defined in Table B.2.

Variable	Description	Units	Source
a_7	Shear velocity coefficient	-	Input parameter
a_8	Entrainment coefficient	s^2 kg^{-1}	Input parameter
a_9	Bank erosion scaling factor	kg m^{-2} m^{-3} s day^{-1}	Input parameter
a_{10}	Bank erosion nonlinear coefficient	-	Input parameter
a_D	Gradient (grain size vs velocity)	s	Constant (9.99)
b_D	Power (grain size vs velocity)	-	Constant (2.52)
D_{low}	Smallest diameter of the sediment class	m	Clay: 0 Silt: 2×10^{-6} Fine sand: 6×10^{-5} Medium sand: 2×10^{-4} Coarse sand: 6×10^{-4}
D_{max}	Maximum entrainable grain size	m	Equation B-16
D_{med}	Median grain size of the sediment class	m	Equation B-22
d_{reach}	Reach depth	m	Equation A-22
D_{upp}	Largest diameter of the sediment class	m	Clay: 2×10^{-6} Silt: 6×10-5 Fine sand: 2×10^{-4} Medium sand: 6×10^{-4} Coarse sand: 2×10^{-3}
f	Friction factor	-	Equation B-19
g	Gravitational acceleration	m s^{-2}	Constant (9.8)
L_{reach}	Reach length	m	Input parameter
$m_{bed,areal}$	Mass of bed sediment per unit area	kg m^{-2}	Equation B-23
M_{bed}	Mass of bed sediment in the reach	kg	Equation B-24
m_{dep}	Mass of sediment deposited on the stream bed	kg m^{-2} day^{-1}	Equation B-20
M_{eff}	Sediment mass discharged by point sources	kg day^{-1}	Equation B-10
m_{ent}	Mass of sediment entrained per unit area	kg m^{-2} day^{-1}	Equation B-14
$M_{land,z}$	Sediment entering the reach per grain size class	kg day^{-1}	Equation B-7
m_{prop}	Proportion of sediment that can be entrained	-	Equation B-17
m_{rel}	Clay release from channel banks	kg m^{-2} day^{-1}	Equation B-11
M_{SS}	Mass of suspended sediment in the reach	kg	Equation B-9
$M_{SS,out}$	Mass of sediment transported from the reach	kg day^{-1}	Equation B-13
M_{US}	Mass of sediment delivered from upstream	kg day^{-1}	Equation B-12
μ	Fluid viscosity	kg m^{-1} s^{-1}	Constant (0.001)
ω	Stream power per unit area	J s^{-1} m^{-2}	Equation B-18
q_{eff}	Effluent flow rate	m^3 s^{-1}	Input time series/parameter
$q_{reach,out}$	Reach discharge	m^3 s^{-1}	Equation A-18
ρ_s	Sediment density	kg m^{-3}	Constant (2650)
ρ_w	Density of water	kg m^{-3}	Constant (1000)
S_{eff}	Suspended sediment concentration in effluent	mg l^{-1}	Input time series/parameter
s_{reach}	Energy slope ≈ mean channel slope	-	Input parameter
u_T	Settling velocity	m s^{-1}	Equation B-21
v	In-stream flow velocity	m s^{-1}	Equation A-21
v^*	Shear velocity	m s^{-1}	Equation B-15
V_{reach}	Reach water volume	m^3	Equation A-19
w_{reach}	Reach width	m	Input parameter

Table B.2: Variables used in in-stream sediment equations

B.2.1 Suspended sediment

For each grain size class, the change in suspended sediment mass with time (Equation B-9) depends on the difference between sediment inputs and outputs. Inputs are from the terrestrial compartment (Equation B-7), sewage or industrial effluent (Equation B-10), clay erosion from channel banks (Equation B-11), any upstream reaches (Equation B-12), and entrainment from the stream bed (Equation B-14); outputs are via outflow from the reach (Equation B-13) and sediment deposition (Equation B-20).

Equation B-9: Change in suspended sediment mass, M_{SS}, with time (kg day^{-1})

$$\frac{dM_{SS}}{dt} = M_{land,z} + M_{eff} + M_{US} - M_{SS,out} + L_{reach}\, w_{reach}\left(m_{ent} + m_{rel} - m_{dep}\right)$$

Equation B-10: Reach sediment inputs from point sources, M_{eff} (kg day^{-1})

$$M_{eff} = 86.4\, q_{eff} S_{eff}$$

Equation B-11: Clay release from channel banks per unit area, m_{rel} (kg m^{-2} day^{-1})

$$m_{rel} = a_9\left(q_{reach,out}\right)^{a_{10}}$$

Equation B-12: Mass of sediment delivered from upstream, M_{US} (kg day^{-1})

If reach = 1: $M_{US} = 0$

Otherwise: $M_{US}^{reach=i} = M_{SS,out}^{reach=(i-1)}$

Equation B-13: Reach suspended sediment outflow, $M_{SS,out}$ (kg day^{-1})

$$M_{SS,out} = 86400\, \frac{M_{SS}}{V_{reach}}\, q_{reach,out}$$

B.2.2 Sediment entrainment

Sediment entrainment is given by Equation B-14. The first step in this calculation is to estimate shear velocity (Equation B-15), which is then used to estimate the maximum entrainable grain size using an empirical relationship (Equation B-16). The maximum entrainable grain size is then used to determine the proportion of the stream bed sediment that can be entrained for the given shear velocity (Equation B-17). Entrainment also depends on stream power, assuming a rectangular cross-section (Equation B-18), and a friction factor (Equation B-19), which represents the hydraulic characteristics of the channel.

Equation B-14: Mass of sediment entrained per unit area, m_{ent} (kg m^{-2} day^{-1}) (N.B. for unit balance: 1 J = 1 kg m^2 s^{-2})

$$m_{ent} = 86400\, a_8\, m_{bed,areal}\, m_{prop}\, \omega f$$

Equation B-15: Shear velocity, v^* (m s^{-1}): $v^* = \sqrt{g\ d_{reach}\ a_7\ s_{reach}}$

Equation B-16: Maximum entrainable grain size, D_{max} (m): $D_{max} = a_D(v^*)^{b_D}$

Equation B-17: Proportion of the sediment that can be entrained for a given shear velocity, m_{prop} (range 0-1)

If $D_{max} < D_{low}$: $m_{prop} = 0$

If $D_{max} > D_{upp}$: $m_{prop} = 1$

Otherwise: $m_{prop} = \dfrac{D_{max} - D_{low}}{D_{upp} - D_{low}}$

Equation B-18: Stream power per unit area, ω (J s^{-1} m^{-2}): $\omega = \rho_w g s_{reach} v\ d_{reach}$

Equation B-19: The friction factor, f (dimensionless)

$$f = \frac{4d_{reach}}{2d_{reach} + w_{reach}}$$

B.2.3 Sediment deposition

The rate of sediment deposition on the stream bed (Equation B-20) is calculated using the terminal settling velocity, approximated using Stokes' law (Equation B-21). Terminal settling velocity is specific for each sediment size class, using median grain sizes for each class (Equation B-22).

Equation B-20: Mass of sediment deposited on the stream bed per unit area, m_{dep} (kg m^{-2} day^{-1})

$$m_{dep} = 86400\ u_T \left(\frac{M_{SS}}{V_{reach}}\right)$$

Equation B-21: Terminal settling velocity, u_T (m s^{-1})

$$u_T = \frac{(\rho_s - \rho_w) g\ {D_{med}}^2}{18\ \mu}$$

Equation B-22: Median grain size, D_{med} (m)

$$D_{med} = D_{low} + \frac{(D_{upp} - D_{low})}{2}$$

B.2.4 Bed sediment

The change in bed sediment mass per unit area (Equation B-23) is controlled by deposition and entrainment of sediment. The whole reach bed sediment mass is also calculated for use in the phosphorus model (Equation B-24).

Equation B-23: Change in bed sediment mass per unit area, $m_{bed,areal}$, with time (kg m^{-2} day^{-1})

$$\frac{dm_{bed,areal}}{dt} = m_{dep} - m_{ent}$$

Equation B-24: Reach bed sediment mass, $M_{bed,reach}$ (kg): $M_{bed} = L_{reach}\ w_{reach} m_{bed,areal}$

Appendix C Snow module and soil temperature

For regions with significant winter snow accumulation, a snow module provides an estimate of snow depth, for use in soil temperature calculations, and of snow melt, which may be used when calculating infiltration rate (Equation A-10). Snow module equations are described more fully in Rankinen et al. (2004b). Briefly, snow depth in water equivalents is calculated as a function of inputs minus outputs (Equation C-1) and then converted to actual snow depth (Equation C-2). Inputs are precipitation falling as snow (Equation C-3), which is calculated by comparing air temperature to two temperature thresholds – the temperature at which rain starts falling as snow, and the temperature at which all rain falls as snow. Outputs are snowmelt (Equation C-4) and evaporation (Equation C-5). Parameters and variables in the snow equations are defined in Table C.1.

Equation C-1: Snow depth in water equivalents, $d_{snow,weq}$ (mm), where superscript *t* denotes the current time step, and *t-1* the previous time step

$$d^{t}_{snow,weq} = d^{t-1}_{snow,weq} + R_{snow} - S_{Melt} - S_{Evap}$$

On the first time step: $d^{t-1}_{snow,weq} = d_{snow,weq,0}$

Equation C-2: Snow depth, d_{snow} (cm)

$$d_{snow} = \frac{1}{F_W}\frac{d_{snow,weq}}{10}$$

Equation C-3: Precipitation falling as snow, R_{snow} (mm day^{-1})

$$if\ T_{air} \geq T_{rain}: R_{snow} = 0$$

$$if\ T_{snow} < T_{air} < T_{rain}: R_{snow} = C_s R_{actual}\frac{(T_{rain} - T_{air})}{(T_{rain} - T_{snow})}$$

$$if\ T_{air} \leq T_{snow}: R_{snow} = C_s R_{actual}$$

Equation C-4: The depth of water lost from the snowpack through snowmelt, S_{Melt} (mm day^{-1})

$$S_{Melt} = \text{minimum}\{F_M(T_{air} - T_{melt}), d_{snow,weq}\}$$

Equation C-5: Evaporation from the snowpack, S_{Evap} (mm day^{-1})

$$S_{Evap} = \text{minimum}\{R_{snow}, S_{PEvap}\}$$

Variable	Description	Units	Source
C_s	Snowfall correction factor	-	Constant (1.23)
d_{snow}	Snow depth	cm	Equation C-2
$d_{snow,weq}$	Snow depth (water equivalents)	mm	Equation C-1
$d_{snow,weq,0}$	Initial snow depth (water equivalents)	mm	Input parameter
F_M	Degree day factor for snowmelt	mm $^oC^{-1}$ day^{-1}	Input parameter
F_W	Water equivalent factor	-	Input parameter
R_{actual}	Measured precipitation	mm day^{-1}	Input time series
R_{snow}	Precipitation falling as snow	mm day^{-1}	Equation C-3
S_{Evap}	Water lost to evaporation	mm day^{-1}	Equation C-5
S_{Melt}	Snowmelt	mm day^{-1}	Equation C-4
S_{PEvap}	Potential snow evaporation rate	mm day^{-1}	Constant (0.09)
T_{air}	Air temperature	°C	Input time series
T_{melt}	Snow melt temperature	°C	Constant (0.5)
T_{rain}	Temperature above which all precipitation falls as rain	°C	Constant (1)
T_{snow}	Temperature below which all precipitation falls as snow	°C	Constant (-1.5)

Table C.1: Variables and parameters used in the snow pack equations.

Soil temperature is calculated from air temperature using a model developed by Rankinen et al. (2004a), taking the insulating effect of snow cover into account (Equation C-6; variables defined in Table C.2).

Equation C-6: Soil temperature at 20 cm depth, T_{soil} (°C), where superscript *t* denotes the current time step, *t-1* the previous time step, and Δt the time step (1 day)

$$T_{soil}^{t} = \left(T_{soil}^{t-1} + \frac{86400\ \Delta t\ K_T}{10^6 C_a \left(2d_{soil,temp}\right)^2} \left(T_{air}^{t-1} - T_{soil}^{t-1}\right) \right) e^{-f_{snow} d_{snow}}$$

$$\text{If } T_{soil}^{t-1} > 0\text{: } C_a = C_{soil}\text{; otherwise: } C_a = C_{soil} + C_{freeze}$$

Variable	Description	Units	Source
$C_{freezethaw}$	Specific heat capacity due to freezing and thawing	10^6 J m^{-3} $°C^{-1}$	Input parameter
C_{soil}	Specific heat capacity of soil	10^6 J m^{-3} $°C^{-1}$	Constant (1.1)
d_{snow}	Snow depth	cm	Equation C-2
$d_{soil,temp}$	Depth at which soil temperature is calculated	m	Constant (0.2)
f_{snow}	Empirical damping parameter	cm^{-1}	Input parameter
K_t	Soil thermal conductivity	W m^{-1} $°C^{-1}$	Input parameter
T_{air}	Air temperature	°C	Input time series
T_{soil}	Soil temperature	°C	Equation C-6

Table C.2: Variables and parameters used in the soil temperature calculation.

Appendix D In-stream biomass equations

A full description of the underlying scientific basis for the in-stream biological equations in INCA-P is provided by Wade et al. (2002a). Briefly, epiphytic algae may remove TDP from the water column, whilst macrophytes may remove TDP from stream bed porewaters. TDP uptake by epiphytic algae depends on the epiphyte growth rate, which in turn depends on the biomass of epiphytic algae (Equation D-1). The change in epiphyte biomass with time is therefore tracked, and is a function of the growth rate (Equation D-2) and the death rate (Equation D-3). Epiphytic algae use macrophytes as their substrate, so epiphyte growth rate also depends on macrophyte biomass (Equation D-4). As with epiphytes, the change in macrophyte biomass with time depends on the growth rate (Equation D-5) and the death rate (Equation D-6). All parameters and variables in the in-stream biomass equations are defined in Table D.1.

Equation D-1: Change in epiphyte biomass, M_E, with time (g C m^{-2} day^{-1})

$$\frac{dM_E}{dt} = B_{growth,epi} - B_{death,epi}$$

Equation D-2: Epiphyte growth rate, $B_{growth,epi}$ (g C m^{-2} day^{-1})

$$B_{growth,epi} = \frac{C_{15}\,\theta_E^{(T_{water}-20)} M_E M_M R_{solar}\ TDP_{wc}}{(C_{16} + TDP_{wc})}$$

Equation D-3: Epiphyte death rate, $B_{death,epi}$ (g C m^{-2} day^{-1})

$$B_{death,epi} = C_{17} M_E q_{reach,out}$$

Equation D-4: The change in macrophyte biomass, M_M, with time (g C m^{-2} day^{-1})

$$\frac{dM_M}{dt} = B_{growth,mac} - B_{death,mac}$$

Equation D-5: Macrophyte growth rate, $B_{growth,mac}$ (g C m^{-2} day^{-1})

$$B_{growth,mac} = \frac{C_{11}\theta_M^{(T_{water}-20)} M_M\ R_{solar}\ C_{12}\ TDP_{pw}}{(C_{13} + TDP_{pw})(C_{12} + M_M)}$$

Equation D-6: Macrophyte death rate, $B_{death,mac}$ (g C m^{-2} day^{-1})

$$B_{death,mac} = C_{14} M_E M_M\ q_{reach,out}$$

Growth rates of both epiphytes and macrophytes are dependent on stream temperature (Equation D-7), which is calculated as a function of air temperature as in Sælthun (1996), and on solar radiation (Equation D-8). Daily mean photosynthetically available solar radiation is calculated based on reach latitude and longitude, using equations originally sourced for B. Cox's PhD thesis (University of Reading). Solar radiation is initially calculated as a 30 minute time series using an equation simplified from Coulson (1975). This is then re-sampled to a daily mean value for use in INCA-P's in-stream biomass equations. The solar radiation equation requires the calculation of an atmospheric adsorption factor, derived using equations described in Bras (1990). It also requires an estimate of solar elevation throughout the day (Equation D-8). This varies throughout the year as solar declination changes (the angle of the Earth's tilt relative to the sun). Solar declination is

calculated using equations from Kirk (1994). Finally, solar radiation is set to zero outside daylight hours through the use of a daylight hours factor, $f_{daylight}$, set to 1 during daylight hours. Daylight hours are calculated from the times of sunrise and sunset, in turn calculated using equations from Meeus (1998) using reach latitude and longitude.

Equation D-7: In-stream water temperature, T_{water} (°C). Superscript *t* denotes the current time step, *t-1* the previous time step. The temperature on the first day is a user-supplied parameter.

$$T_{water}^{t=0} = T_{water,0}$$

$$T_{water}^{t>0} = \frac{C_{lag} - 1}{C_{lag}} T_{water}^{t-1} + \frac{1}{C_{lag}} maximum\{T_{air}^{t}, T_{water,min}\}$$

Equation D-8: Photosynthetically available solar radiation as a daily mean, $R_{solar,daily}$ (W m^{-2}), expressed in pseudo-code

$$R_{solar,daily} = resample\left(R_{solar,30mins}; frequency = daily, how = mean\right),$$

where $R_{solar,30mins} = S_0 A_{ads} \sin \beta_{solar} f_{daylight}$

Equation D-9: Solar elevation, β_{solar} (°): $\sin \beta_{solar} = \sin \gamma_{lat} \sin \delta - \cos \gamma_{lat} \cos \delta \cos \tau$

Variable	Description	Units	Source
A_{ads}	Atmospheric solar radiation adsorption factor	-	Model calculates
β_{solar}	Solar elevation	°	Equation D-9
$B_{death,epi}$	Epiphyte death rate	g C m^{-2} day^{-1}	Equation D-3
$B_{death,mac}$	Macrophyte death rate	g C m^{-2} day^{-1}	Equation D-6
$B_{growth,epi}$	Epiphyte growth rate	g C m^{-2} day^{-1}	Equation D-2
$B_{growth,mac}$	Macrophyte growth rate	g C m^{-2} day^{-1}	Equation D-5
C_{11}	Macrophyte growth rate coefficient	day^{-1}	Input parameter
C_{12}	Self-shading for macrophytes	g C m^{-2}	Input parameter
C_{13}	Half saturation of P for macrophyte growth	mg l^{-1}	Input parameter
C_{14}	Macrophyte death rate coefficient	s m^{-1} g C^{-1} day^{-1}	Input parameter
C_{15}	Epiphyte growth rate coefficient	m^2 g C^{-1} day^{-1}	Input parameter
C_{16}	Half saturation of P for epiphyte growth	mg l^{-1}	Input parameter
C_{17}	Epiphyte death rate coefficient	s m^{-3} day^{-1}	Input parameter
C_{lag}	Water temperature lag factor	-	Input parameter
δ	Solar declination	°	Model calculates
$f_{daylight}$	Daylight hours factor (0 or 1)	-	Model calculates
γ_{lat}	Latitude	°	Input parameter
M_E	Epiphyte biomass	g C m^{-2}	Equation D-1
M_M	Macrophyte biomass	g C m^{-2}	Equation D-4
$q_{reach,out}$	Reach outflow	m^3 s^{-1}	Equation A-18
R_{solar}	Normalised solar radiation	-	Equation D-8
S_0	Solar constant	W m-2	Constant (1378)
T_{air}	Air temperature	°C	Input time series
T_{water}	Water temperature	°C	Equation D-7
$T_{water,0}$	Initial water temperature	°C	Input parameter
$T_{water,min}$	Minimum water temperature	°C	Input parameter
TDP_{pw}	Porewater TDP concentration	mg l^{-1}	Equation 35
TDP_{wc}	Water column TDP concentration	mg l^{-1}	Equation 24
θ_E	Epiphyte temperature dependency	-	Input parameter
θ_M	Macrophyte temperature dependency	-	Input parameter
τ	Time of day expressed as an angle	°	Model calculates

Table D.1: Variables and parameters used in in-stream biomass equations.

Appendix E Initial conditions

Ordinary differential equations (ODEs) are used to describe the rate of change in volume or mass of model state variables with respect to time. These ODEs are then solved numerically. To do this, initial conditions must be provided for each state variable. A summary of the state variables in the model with associated ODEs is provided in Table E.1, together an explanation for how initial conditions are derived. Where initial conditions are calculated by the model using additional parameters, these are defined in Table E.2.

Type	Variable	Description	Source of initial conditions
P	$P_{TDP,soil}$	Soil water TDP mass	$P_{TDP,soil} = 10^{-3}(V_{soil\_drainage} + V_{soil\_ret})\ \mathrm{TDP}_{soil,0}$
	$P_{labile,soil}$	Labile soil P mass	$P_{labile,soil} = 10^{-6} M_{soil}\, P_{conc,labile,0}$
	$P_{inactive,soil}$	Inactive soil P mass	$P_{inactive,soil} = 10^{-6} M_{soil}\, P_{conc,inactive,0}$
	$P_{TDP,gw}$	Groundwater TDP mass	$P_{TDP,gw} = 10^{-3} V_{gw}\ \mathrm{TDP}_{gw,0}$
	$P_{sorbed,gw}$	Aquifer sorbed P mass	$P_{sorbed} = 10^{3} m_{aquifer,areal}\, P_{conc,gw,0}$
	$P_{TDP,quick}$	Quick flow TDP mass	$P_{TDP,quick} = 10^{-3} V_{quick}\ \mathrm{TDP}_{quick,0}$
	$P_{TDP,land}$	TDP delivery to the reach	$P_{TDP,land} = 86400\left(\frac{q_{soil\_out}\, P_{TDP,soil}}{V_{soil\_drainage} + V_{soil\_ret}} + \frac{q_{gw}\, P_{TDP,gw}}{V_{gw}} + \frac{q_{quick}\, P_{TDP,quick}}{V_{quick}}\right)$
	$P_{TDP,wc}$	Water column TDP mass	$P_{TDP,wc} = 10^{-3}\mathrm{TDP}_{wc,0}\, V_{reach}$
	$P_{sorbed,wc}$	Water column adsorbed P mass	$P_{sorbed,wc} = P_{PP,wc} = 10^{-3}\mathrm{PP}_{wc,0}\, V_{reach}$
	$P_{TDP,pw}$	Stream bed pore water TDP mass	$P_{TDP,pw} = 10^{-3}\mathrm{TDP}_{pw,0}\, w_{reach}\, L_{reach}\, d_{bed}\, \theta_{bed}$
	$P_{PP,wc}$	Water column PP mass	$P_{sorbed,wc} = P_{PP,wc} = 10^{-3}\mathrm{PP}_{wc,0}\, V_{reach}$
	$P_{PP,bed}$	Stream bed sediment PP mass	$P_{PP,bed} = L_{reach}\, w_{reach}\mathrm{PP}_{bed,0} \sum_{z=\text{grain size}} m^{z}_{bed,areal}$ where superscript z is one of 5 grain size classes
H	q_{soil_out}	Soil water flow	Input parameter
	$V_{soil\_drainage}$	Soil water drainage volume	$V_{soil\_drainage} = 86400 q_{soil\_out}\, T_{soil}$
	q_{quick}	Quick flow	Input parameter
	V_{quick}	Quick flow volume	$V_{quick} = 86400\ q_{quick}\, T_{quick}$
	q_{gw}	Groundwater flow	Input parameter
	V_{gw}	Groundwater volume	$V_{gw} = 10^{6} d_{aquifer} C_{7}$
	$q_{reach,out}$	Reach flow	Reach 1: Input parameter Reach >1: Equivalent to the simulated outflow from the reach upstream at the end of the first time step
	V_{reach}	Reach volume	$V_{reach} = 86400\ T_{reach}\ q_{reach,out}$ where $T_{reach} = \frac{L_{reach}}{86400\ a q^{b}_{reach,out}}$
S	S_{store}	Surface sediment store	Input parameter
	M_{soil}	Soil mass	$M_{soil} = 10^{6} d_{soil}\, \rho_{bulk,soil}$
	M_{SS}	Water column SS mass	For each grain size class: $M_{SS} = 10^{-3}(SS_0)V_{reach}$
	$M_{bed,areal}$	Stream bed sediment mass	Five input parameters (one per grain size class)
B	M_E	Epiphyte biomass	Input parameter
	M_M	Macrophyte biomass	Input parameter

Table E.1: Source of initial conditions for ordinary differential equations solved in INCA-P. The 'type' column refers to phosphorus (P), hydrology (H), sediment (S) or biology (B).

Variable	Description	Units	Source
a	Velocity-discharge a parameter	m^{-2}	Input parameter
b	Velocity-discharge b parameter	-	Input parameter
C_7	Aquifer proportion of pore-filled spaces	-	Input parameter
$d_{aquifer}$	Aquifer depth × porosity	m	Input parameter
d_{bed}	Bed sediment depth	m	Input parameter
d_{soil}	Average depth of the soil in the O/A horizon	m	Input parameter
L_{reach}	Reach length	m	Input parameter
$m_{aquifer,areal}$	Aquifer mass per m^2 (depth × density)	10^3 kg m^{-2}	Input parameter
$P_{conc,gw,0}$	Initial aquifer P ratio	mg P kg $soil^{-1}$	Input parameter
$P_{conc,inactive,0}$	Initial soil inactive P ratio	mg P kg $soil^{-1}$	Input parameter
$P_{conc,labile,0}$	Initial soil labile P ratio	mg P kg $soil^{-1}$	Input parameter
$PP_{bed,0}$	Initial stream bed P: sediment ratio	kg P kg sed^{-1}	Input parameter
$PP_{quick,0}$	Initial quick flow PP concentration	mg l^{-1}	Input parameter
$PP_{wc,0}$	Initial in-stream PP concentration	mg l^{-1}	Reach 1: Input parameter Downstream reaches: set equal to the simulated concentration for the upstream reach at the end of the first time step
$\rho_{bulk,soil}$	Soil bulk density	kg m^{-3}	Input parameter
SS_0	Initial in-stream SS concentration	mg l^{-1}	Five input parameters (one per grain size class)
θ_{bed}	Bed sediment porosity	-	Input parameter
T_{quick}	Quick flow time constant	days	Input parameter
T_{soil}	Soil water time constant	days	Input parameter
$TDP_{gw,0}$	Initial groundwater TDP concentration	mg l^{-1}	Input parameter
$TDP_{pw,0}$	Initial stream bed porewater TDP concentration	mg l^{-1}	Input parameter
$TDP_{quick,0}$	Initial quick flow TDP concentration	mg l^{-1}	Input parameter
$TDP_{soil,0}$	Initial soil water TDP concentration	mg l^{-1}	Input parameter
$TDP_{wc,0}$	Initial water column TDP concentration	mg l^{-1}	Reach 1: Input parameter Downstream reaches: set equal to the simulated concentration for the upstream reach at the end of the first time step
V_{soil_ret}	Soil water retention volume	m^3 km^{-2}	Equation A-6
w_{reach}	Reach width	m	Input parameter

Table E.2: Parameters and variables used to calculate initial conditions.

Appendix F Input parameters

User input parameters are described below (Table F.2 to Table F.5), grouping parameters into separate tables according to whether they are supplied by landscape class, sub-catchment or reach, in which case separate parameter values must be supplied for each landscape class, sub-catchment or reach, respectively. There are also input parameters which affect in-stream processes which are not supplied by reach.

Within each table, parameters are grouped by the processes they relate to as follows: H: hydrology processes, P: phosphorus processes, S: sediment processes, B: in-stream biomass processes, G: general parameters (relating to numerous processes) and snow processes.

For each parameter, an indication is provided of the potential sensitivity of the model to the parameter (the 'Importance' column). This is subjectively derived from experience of the model and knowledge of the model equations. It may however serve to help highlight the key parameters for which particular care is required during model set-up. Parameters are also classed according to 'Data availability', to give an indication of whether parameter values may be based on observations or literature-derived values, or whether they need to be determined purely through calibration. A key to the 'Importance' and 'Data availability' columns is given in Table F.1.

Value	'Importance' column	'Data availability' column
0	Likely to exert little influence on model output	Not measurable; value determined through calibration alone
1	Important in some situations/set-ups	Measurable in principle, but data not generally routinely available
2	Usually important	Measurable and data routinely available

Table F.1: Key to the values used in the parameter 'Importance' and 'Data availability' columns in Tables F.2 to F.5.

Process	Parameter	Description	Units	Importance (0-2)	Data availability (0-2)
Initial (H)	$q_{quick,0}$	Initial quick flow	$m^3\ s^{-1}\ km^{-2}$	0	0
Initial (H)	$q_{soil,0}$	Initial soil water flow	$m^3\ s^{-1}\ km^{-2}$	1	0
Initial (P)	$P_{conc,inactive,0}$	Initial soil inactive P ratio	mg P kg $soil^{-1}$	1	2
Initial (P)	$P_{conc,labile,0}$	Initial soil labile P ratio	mg P kg $soil^{-1}$	2	2
Initial (P)	$PP_{quick,0}$	Initial quick flow PP concentration	mg l^{-1}	0	1
Initial (P)	$TDP_{quick,0}$	Initial quick flow TDP concentration	mg l^{-1}	0	1
Initial (P)	$TDP_{soil,0}$	Initial soil water TDP concentration	mg l^{-1}	1	1
Initial (P,S)	$\rho_{bulk,soil}$	Bulk density of the soil	kg m^{-3}	1	2
Initial (S)	$S_{store,0}$	Initial store of sediment available for transport	kg km^{-2}	1	0
G (H, P, S)	A_{LU}	Area of landscape in sub-catchment	%	2	2
H	C_{ret}	Soil water retention volume constant	-	1	0
H	I_{max}	Maximum infiltration rate	mm day^{-1}	2	1
H	$q_{soil,sus}$	Sustainable soil water flow	$m^3\ s^{-1}\ km^{-2}$	1	0
H	T_{quick}	Quick flow time constant	days	2	0
H	T_{soil}	Soil water time constant	days	2	0
H, P	SMD_{max}	Maximum soil moisture deficit	mm	1	2
P	C_{freeze}	Specific heat capacity due to freeze thaw	$10^6\ J\ m^{-3}\ °C^{-1}$	0	1
P	C_{immob}	Chemical immobilisation factor	day^{-1}	1	0
P	$C_{sat,labile}$	Maximum soil labile P content	kg P kg sed^{-1}	1	1
P	C_{uptake}	Plant P uptake factor	m day^{-1}	2	0
P	$C_{weathering}$	Weathering factor	day^{-1}	1	0
P	d_{soil}	Soil depth in the O/A horizon	m	2	2
P	E_{PP}	PP enrichment factor	-	2	1
P	F_{period}	Fertilizer addition period	days	2	2
P	f_{snow}	Empirical damping parameter	cm^{-1}	0	0
P	F_{start}	Day number when fertilizer addition starts	-	2	2
P	G_{amp}	Plant growth curve amplitude	-	1	0
P	G_{offset}	Plant growth curve vertical offset	-	1	0
P	G_{period}	Growing season length	days	2	2
P	G_{start}	Start of the growing season (day of year)	-	2	2
P	$K_{f,soil}$	Soil P sorption coefficient	l kg $soil^{-1}$	2	1
P	K_{soil}	Soil sorption scaling factor	day^{-1}	2	0
P	K_t	Soil thermal conductivity	W m^{-1} $°C^{-1}$	0	1
P	n_{soil}	Soil Freundlich isotherm constant	-	2	1
P	$P_{liq,fert}$	Liquid fertilizer P inputs	kg ha^{-1} day^{-1}	2	2
P	$P_{liq,manure}$	Liquid manure P inputs	kg ha^{-1} day^{-1}	2	2
P	$P_{maxUptake,day}$	Maximum daily plant P uptake	kg ha^{-1} day^{-1}	2	1
P	$P_{maxUptake,yr}$	Maximum annual plant P uptake	kg ha^{-1} yr^{-1}	2	2
P	$P_{residue}$	Plant residue soil P inputs	kg ha^{-1} day^{-1}	1	1
P	$P_{solid,fert}$	Solid fertilizer P inputs	kg ha^{-1} day^{-1}	2	2
P	$P_{solid,manure}$	Solid manure P inputs	kg ha^{-1} day^{-1}	2	2
P	$T_{immob,0}$	Lower temperature threshold for immobilisation	°C	0	1
P	t_{Q10}	Change in rate with a 10°C change in temperature	-	1	1
P	$t_{Q10,base}$	Temperature at which the rate response is 1	°C	1	1
S	C_{SD}	Splash detachment scaling factor	s m^{-1}	1	0
S	E_{FE}	Flow erosion potential	kg km^{-2} s^{-1}	2	1
S	E_{SD}	Splash detachment soil erodibility	kg m^{-2} s^{-1}	1	1
S	F_{Cl}	Clay fraction	%	1	2
S	F_{CS}	Coarse sand soil fraction	%	1	2
S	F_{FS}	Fine sand fraction	%	1	2
S	F_{MS}	Medium sand soil fraction	%	1	2
S	F_{Si}	Silt fraction	%	1	2
S	V_{index}	Vegetation index	-	1	0
Snow	$d_{snow,weq,0}$	Initial snow depth (water equivalents)	mm	0	2
Snow	F_M	Degree day-factor for snowmelt	mm $^oC^{-1}$ day^{-1}	0	2
Snow	F_W	Water equivalent factor	-	0	2

Table F.2: User input parameters supplied for each landscape class.

Variable	Parameter	Description	Units	Importance (0-2)	Data availability (0-2)
Initial (H)	C_7	Aquifer proportion of pore-filled spaces	-	1	1
Initial (H)	$d_{aquifer}$	Aquifer depth × porosity	m	2	1
Initial (H)	$q_{gw,0}$	Initial groundwater flow	$m^3\ s^{-1}\ km^{-2}$	2	1
Initial (P)	$P_{conc,gw,0}$	Initial aquifer P ratio	mg P kg sed^{-1}	1	1
Initial (P)	$TDP_{gw,0}$	Initial groundwater TDP concentration	mg l^{-1}	2	1
G (H, P, S)	A_{SC}	Sub-catchment area	km^2	2	2
H, P	β	Base flow index	-	2	2
H	$C_{IExcess}$	Infiltration excess proportion to quick flow	-	1	0
H	$q_{gw,sus}$	Groundwater sustainable flow	$m^3\ s^{-1}\ km^{-2}$	1	0
H	$q_{soil,max}$	Threshold soil water flow for saturation excess	$m^3\ s^{-1}\ km^{-2}$	2	0
H	T_{gw}	Groundwater time constant	days	2	0
P	$C_{sat,aquifer}$	Maximum aquifer matrix P:sed ratio	kg P kg sed^{-1}	1	1
P	$K_{f,gw}$	Groundwater P sorption coefficient	l kg $soil^{-1}$	1	1
P	K_{gw}	Groundwater sorption scaling factor	day^{-1}	1	0
P	$m_{aquifer,areal}$	Aquifer mass per m^2 (depth × density)	10^3 kg m^{-2}	1	1
P	n_{gw}	Groundwater Freundlich isotherm constant	-	1	1
P	$P_{dep,solid}$	Annual atmospheric dry P deposition	kg $ha^{-1}\ yr^{-1}$	1	2
P	$P_{dep,wet,annual}$	Annual atmospheric wet P deposition	kg $ha^{-1}\ yr^{-1}$	1	2
S	a_1	Flow erosion scaling factor	$s\ m^{-2}$	2	0
S	a_2	Flow erosion direct runoff threshold	$m^3\ s^{-1}\ km^{-2}$	1	0
S	a_3	Flow erosion non-linear coefficient	-	2	0
S	a_4	Transport capacity scaling factor	kg $m^{-2}\ km^{-2}$	2	0
S	a_5	Transport capacity direct runoff threshold	$m^3\ s^{-1}\ km^{-2}$	1	0
S	a_6	Transport capacity nonlinear coefficient	-	2	0

Table F.3: User input parameters supplied for each sub-catchment.

Variable		Parameter	Description	Units	Importance (0-2)	Data availability (0-2)
General in-stream parameters	Initial (B)	$M_{E,0}$	Initial epiphyte biomass	g C m^{-2}	1	1
	Initial (B)	$M_{M,0}$	Initial macrophyte biomass	g C m^{-2}	1	1
	Initial (P)	$PP_{bed,0}$	Initial stream bed P ratio	kg P kg sed^{-1}	2	1
	Initial (P)	$TDP_{pw,0}$	Initial porewater TDP concentration	mg l^{-1}	0	1
	B	C_{lag}	Water temperature lag factor	-	0	0
	B	$T_{water,0}$	Initial water temperature	°C	0	2
	B	$T_{water,min}$	Minimum water temperature	°C	0	1
	P	$C_{sat,bed}$	Maximum P:sed ratio in the stream bed	kg P kg sed^{-1}	1	1
	P	$C_{sat,wc}$	Maximum P:sed ratio in suspended material	kg P kg sed^{-1}	1	1
	P	c_{SRP}	Regression between TDP and SRP (y-intercept)	mg l^{-1}	1	2
	P	DOC_{wc}	Mean water column DOC concentration	mg l^{-1}	1	2
	P	m_{DOC}	Ratio of dissolved hydrolysable P to DOC	-	1	1
	P	m_{SRP}	Regression between TDP and SRP (gradient)	-	1	2
Reach 1 initial conditions	Initial (H)	$q_{reach,out,0}$	Initial flow out of the reach	$m^3\ s^{-1}$	1	2
	Initial (P)	$PP_{wc,0}$	Initial water column PP concentration	mg l^{-1}	1	1
	Initial (P)	$TDP_{wc,0}$	Initial water column TDP concentration	mg l^{-1}	1	2
	Initial (S)	$SS_{0,Cl}$	Initial SS clay concentration	mg l^{-1}	1	1
	Initial (S)	$SS_{0,CS}$	Initial SS coarse sand concentration	mg l^{-1}	0	1
	Initial (S)	$SS_{0,FS}$	Initial SS fine sand concentration	mg l^{-1}	1	1
	Initial (S)	$SS_{0,MS}$	Initial SS medium sand concentration	mg l^{-1}	0	1
	Initial (S)	$SS_{0,Si}$	Initial SS silt concentration	mg l^{-1}	1	1

Table F.4: User input parameters supplied for the in-stream module (not varied by reach)

Variable	Parameter	Description	Units	Importance (0-2)	Data availability (0-2)
Initial (S)	$m_{bed,areal,0,Cl}$	Initial clay bed sediment mass	kg m^{-2}	1	1
Initial (S)	$m_{bed,areal,0,Si}$	Initial silt bed sediment mass	kg m^{-2}	2	1
Initial (S)	$m_{bed,areal,0,FS}$	Initial fine sand bed sediment mass	kg m^{-2}	1	1
Initial (S)	$m_{bed,areal,0,MS}$	Initial medium sand bed sediment mass	kg m^{-2}	1	1
Initial (S)	$m_{bed,areal,0,CS}$	Initial coarse sand bed sediment mass	kg m^{-2}	1	1
G (H, S)	L_{reach}	Reach length	m	2	2
G (S, H, B)	w_{reach}	Average reach width	m	2	1
H	a	Velocity-discharge a parameter	m^{-2}	2	2
H	b	Velocity-discharge b parameter	-	2	2
H, P	q_{abs}	Abstraction rate	m^3 s^{-1}	1	2
H, P, S	q_{eff}	Effluent discharge	m^3 s^{-1}	2	2
P	d_{bed}	Bed sediment depth	m	1	1
P	$E_{pw,wc}$	Fraction exchanged with stream bed	day^{-1}	1	0
P	$K_{f,pw}$	Pore water sorption coefficient	l kg sed^{-1}	1	1
P	$K_{f,wc}$	Water column sorption coefficient	l kg $soil^{-1}$	1	1
P	K_{pw}	Stream bed porewater sorption scaling factor	day^{-1}	1	0
P	K_{wc}	Water column sorption scaling factor	day^{-1}	1	0
P	n_{pw}	Pore water Freundlich isotherm constant	-	1	1
P	n_{wc}	Water column Freundlich isotherm constant	-	1	1
P	PP_{eff}	Effluent PP concentration	mg l^{-1}	1	2
P	TDP_{eff}	Effluent TDP concentration	mg l^{-1}	2	2
P	θ_{bed}	Bed sediment porosity	-	1	1
S	a_{10}	Bank erosion nonlinear coefficient	-	1	0
S	a_7	Shear velocity coefficient	-	2	0
S	a_8	Entrainment coefficient	s^2 kg^{-1}	2	0
S	a_9	Bank erosion scaling factor	kg m^{-2} m^{-3} s day^{-1}	1	0
S	$S_{eff,Cl}$	Clay concentration in effluent	mg l^{-1}	1	2
S	$S_{eff,Si}$	Silt concentration in effluent	mg l^{-1}	1	2
S	$S_{eff,FS}$	Fine sand concentration in effluent	mg l^{-1}	1	1
S	$S_{eff,MS}$	Medium sand concentration in effluent	mg l^{-1}	0	1
S	$S_{eff,CS}$	Coarse sand concentration in effluent	mg l^{-1}	0	1
S	s_{reach}	Energy slope ≈ mean channel slope	-	2	2
B	C_{11}	Macrophyte growth rate coefficient	day^{-1}	1	0
B	C_{12}	Self-shading for macrophytes	g C m^{-2}	1	0
B	C_{13}	Half saturation of P for macrophyte growth	mg l^{-1}	1	1
B	C_{14}	Macrophyte death rate coefficient	s m^{-1} g C^{-1} day^{-1}	1	0
B	C_{15}	Epiphyte growth rate coefficient	m^2 g C^{-1} day^{-1}	1	0
B	C_{16}	Half saturation of P for epiphyte growth	mg l^{-1}	1	1
B	C_{17}	Epiphyte death rate coefficient	s m^{-3} day^{-1}	1	0
B	$C_{P,epi}$	Proportion of P in epiphytes	g P g C^{-1}	1	1
B	$C_{P,mac}$	Proportion of P in macrophytes	g P g C^{-1}	1	1
B	γ_{lat}	Latitude	°	0	2
B	γ_{long}	Longitude	°	0	2
B	θ_E	Epiphyte temperature dependency	-	0	0
B	θ_M	Macrophyte temperature dependency	-	0	0

Table F.5: User input parameters supplied for each reach.